PERCEPTION OF BUILT ENVIRONMENTS AND ITS NEURAL MODULATION BY THE BEHAVIORAL GOALS OF THE PERCEIVER

A THESIS SUBMITTED TO
THE GRADUATE SCHOOL OF ENGINEERING AND SCIENCE
OF BILKENT UNIVERSITY
IN PARTIAL FULFILLMENT OF THE REQUIREMENTS FOR
THE DEGREE OF
MASTER OF SCIENCE
IN
NEUROSCIENCE

By
Aysu Nur KOÇ
July 2023

PERCEPTION OF BUILT ENVIRONMENTS AND ITS NEURAL MODULATION BY THE BEHAVIORAL GOALS OF THE PERCEIVER
By Aysu Nur KOÇ
July 2023

We certify that we have read this thesis and that in our opinion it is fully adequate, in scope and in quality, as a thesis for the degree of Master of Science.

Yasemin Afacan(Advisor)

Burcu Ayşen Ürgen(Co-Advisor)

Ausaf Ahmed Farooqui

Murat Perit Çakır

Approved for the Graduate School of Engineering and Science:

Orhan Arıkan
Director of the Graduate School

ABSTRACT

PERCEPTION OF BUILT ENVIRONMENTS AND ITS NEURAL MODULATION BY THE BEHAVIORAL GOALS OF THE PERCEIVER

Aysu Nur KOÇ
M.S. in Neuroscience
Advisor: Yasemin Afacan
Co-advisor: Burcu Ayşen Ürgen
July 2023

A scene is a view of an environment with a spatial layout one can act within. Scene perception has been studied extensively in the neuroscience literature, examining changes in neural activity across the brain and scene-selective regions (PPA, RSC, OPA), in response to various low and high-level features and tasks. The focus of the field has been mostly on outdoor scenes based on broad categorical differences (e.g. natural/man-made) or basic differences between otherwise similar indoor environments (e.g. ceiling height) and behavioral components regarding scene perception have been overlooked. Interactions with fields such as environmental psychology or neuroarchitecture, which could inspire a more ecologically valid study of scenes, are rare. Hereby, we investigated the perception of built environments where we spend most of our time, drew our categorization method from the architecture literature, and employed multiple tasks. The categories were elements that (i) allow our access to and circulation within environments (entrances, exits, corridors, stairs); and that (ii) do not directly aid locomotion but rather serve human needs (restrooms, eating and seating areas). FMRI scans were obtained from 23 participants as they viewed scenes from built environments and performed two tasks: a categorization task based on the main afforded action differences between the defined categories, and an approach-avoidance task where participants decided to enter the scene or not, measuring the initial action regarding an environment. Scene-selective ROIs were defined with a localizer session. Univariate analyses did not reveal strong differences between the tasks. Searchlight MVPA revealed categories, but not tasks, are classified at the whole-brain level, at the lingual and parahippocampal gyri, the SMA, and the occipital cortex. Model-based RSA at the ROI level revealed that tasks modulate activation patterns to built environments in all three ROIs, but do not entirely explain them, whereas categorical and visual models did not correlate with the activation patterns in any of these regions. We utilize an interdisciplinary perspective to scene perception to expand the ecological validity of the stimuli and task content, showing that neural responses to built environments are modulated by the behavioral goals of the observer at the ROI level, and stimulus category at the whole-brain level.

Keywords: scene perception, fMRI, PPA, OPA, RSC, RSA, MVPA, neuroarchitecture.

ÖZET

YAPILI ÇEVRELERİN ALGISI VE BUNLARIN GÖZLEMCİNİN DAVRANIŞSAL AMAÇLARI DOĞRULTUSUNDA NÖRAL MODÜLASYONU

Aysu Nur KOÇ
Nörobilim, Yüksek Lisans
Tez Danışmanı: Yasemin Afacan
İkinci Tez Danışmanı: Burcu Ayşen Ürgen
Temmuz 2023

Sahne, kişinin içinde hareket edebileceği uzamsal bir düzene sahip bir ortamın görünümüdür. Sinirbilim literatüründe sahne algısı, tüm beyinde ve sahnelere duyarlı bölgelerde (Parahipokampal yer bölgesi, Retrosplenial korteks, Oksipital yer bölgesi), çeşitli uyaran özelliklerine ve davranışsal görevlere bağlı olarak derinlemesine incelenmiştir. Alanın odağı, geniş kategorik farklılıklara (örneğin doğal/insan yapımı) dayalı olarak çoğunlukla dış mekan sahneleri veya basit farklılıkları olan (örneğin tavan yüksekliği) ve diğer yönleriyle birbirine benzeyen iç mekan sahneleri olmuştur, ve sahne algısını etkileyebilecek davranışsal bileşenler sınırlı kapsamda çalışılmıştır. Sahnelerin ekolojik olarak daha geçerli çalışmasına ilham verebilecek çevresel psikoloji veya nöromimari gibi alanlarla etkileşimler az görülmektedir. Bu çalışmada, zamanımızın çoğunu geçirdiğimiz iç mekanların (yapılı çevreler) algısını araştırdık, sınıflandırma yöntemimizi mimarlık literatüründen uyarladık ve birden fazla davranışsal görev kullandık. Kategoriler, (i) ortamlara erişimimizi ve içinde dolaşımımızı sağlayan (girişler, çıkışlar, koridorlar, merdivenler); ve (ii) bir yerden bir yere hareketten ziyade insan ihtiyaçlarına hizmet eden (tuvaletler, yemek yeme ve oturma alanları) elemanlar olarak belirlendi. 23 katılımcının iMRG taramaları, onlar yapılı çevre kategorilerine ait uyaranlara bakarak iki farklı davranışsal görevi yerine getirirken gerçekleştirildi. Bunlar, katılımcının uyaranları belirlediğimiz kategorilere ayırdığı bir kategorizasyon görevi, ve gördükleri mekana girip girmemeye karar verdikleri, ve bir mekana dair ilk eylemlerini ölçtüğümüz bir yaklaşma/kaçınma göreviydi. Sahne-seçici bölgeler ayrı bir oturum ile belirlendi. Tek değişkenli analizlerin sonucu görevler arasında güçlü farklılılar ortaya çıkarmadı. Tüm beyinde yapılan çok değişkenli sınıflandırma analizi, lingual ve parahipokampal giruslar, supplementer motor alan, ve oksipital korteksteki aktivite örüntülerinin yapılı çevre kategorilerini başarılı bir şekilde ayırt edebildiğini görterdi. Model tabanlı Temsili Benzerlik Analizi (TBA) ise davranışsal görevlerin tüm sahne-seçici alanlardaki aktiviteyi modüle ettiğini, fakat aktivite örüntülerini tamamen açıklayamadığını ortaya koydu. Bu çalışmada disiplinlerarası bir yaklaşım benimseyerek, uyaranlar ve davranışsal görevler açısından sahne algısının ekolojik geçerliliğini genişletmeyi amaçlıyor, ve yapılı çevrelerin algısında nöral aktivite örüntülerinin tüm beyin düzeyinde kategori, sahne-seçici bölgeler düzeyinde ise gözlemcinin davranışsal amaçları tarafından modüle edildiğini gösteriyoruz.

Anahtar sözcükler: sahne algısı, iMRG, PPA, OPA, RSC, temsili benzerlik analizi, nöromimari.

Acknowledgement

I would like to express my deepest gratitude to all those who have contributed to the completion of this thesis.

First and foremost, I would like to thank my supervisors, Assoc. Prof. Yasemin Afacan and Asst. Prof. Burcu Ayşen Ürgen. Your unwavering support and invaluable guidance have been instrumental in shaping the direction and enhancing the quality of this work, and I am glad to have taken my first steps as a researcher with you. I also thank my jury committee, Dr. Ausaf A. Farooqui and Dr. Murat P. Çakır, for their valuable feedback.

I am thankful to my family for supporting and encouraging my education. Especially my mother; her love and trust have been the foundation of my success, and her sacrifices throughout my life made this degree possible.

To my close friends and lab mates Aslı, Sena, and Hüseyin, I extend my sincere appreciation. Your friendship, thought-provoking discussions, and willingness to share knowledge have been of tremendous support. And the one closest to me, Barış, thank you for the countless conversations, shared laughter, and night study sessions; you brightened the times that would otherwise be filled with gloom.

I must also thank all the components of Bilkent, UMRAM, and CCNLab for creating this stimulating research environment. I appreciate our lab members and assistants for their support and for their interest in science.

Lastly, I cannot forget my feline companion, Puding. Your adorable presence, purrs, and amusing antics provided much-needed stress relief during the challenging moments of this thesis. Your companionship brought joy to my days.

Before concluding, I want to thank the Scientific and Technological Research Council of Turkey (TÜBİTAK) for making this project possible, with a 1002-A(122K706) fund and a BIDEB 2210-A scholarship.

Contents

List of Figures

List of Tables

Chapter 1

Introduction

1.1 Scene Perception

Scene perception is a field of study within visual perception, and is concerned with how humans or non-human animals perceive excerpts or snapshots of environments called *scenes*. There are several popular definitions of a *scene* in the literature that mainly refer to a view of the world with a spatial structure that contains objects, but they vary and emphasize different properties depending on the field of research. One classical definition is that scenes are the semantically coherent and spatially organized sums of large background elements like mountains or walls, and smaller discrete elements like furniture or other objects in an environment that are of human scale [1]. Other definitions do not emphasize the coherence or meaning of a scene, but rather define it as a view of the world with spatial elements that may contain items; even room-like structures built with Lego blocks [2]. In general, any view of the world or virtually generated environment that creates a sense of being a place that one can *act within* may be regarded as a scene [3]. The impressive ability of the human brain to process the incredible amount of information regarding our environment even at a glance is often attributed to evolutionary mechanisms; correctly identifying our surroundings and acting accordingly holds crucial survival value to be able to find food, shelter, and avoid threats [4].

Virtually any topic regarding human cognition could benefit from the study of scene perception, as we usually perform actions throughout our lives within various familiar or novel contexts and environments, rather than an isolated experimental setting [5]. Thus scene perception is strongly intertwined with actions such as visual search, navigation, object manipulation, and social behavior, through cognitive processes such as perception, learning, memory, and attention.

This immense impact of scenes and their properties on human cognition and behavior inspired a large body of psychological and neuroscientific research to understand the mechanisms underlying scene perception. Further, findings and methodological advances in scene perception also hold value for rather applied fields such as environmental psychology and more recently neuroarchitecture, that aim to improve human experience. These fields incorporate more and more psychological and neuroscientific findings to detect elements that impact human cognition negatively or positively, and to design better spaces for various human needs.

1.2 Neural Bases of Scene Perception

With the use of neuroimaging techniques, changes in brain activation patterns to various scene properties have been studied meticulously and three scene-selective regions that preferentially respond to scenes compared to other categories of stimuli have been identified in the human brain. These are called parahippocampal place area (PPA), retrosplenial cortex or recently medial place area (RSC), and occipital place area (OPA), as illustrated in Figure 1.1. Results of various experimental paradigms and stimulus properties used in the literature indicate that these areas, although all scene-selective and functionally connected to each other, differ in terms of their roles in scene perception and related processes.

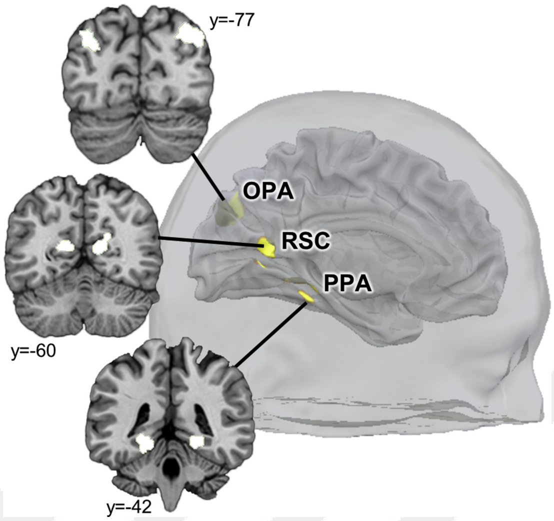

Figure 1.1: **Locations of three scene-selective areas.** Reused with permission [6]

.

1.2.1 Parahippocampal Place Area

The parahippocampal place area (PPA) is located bilaterally in the posterior part of the parahippocampal gyrus, which surrounds the hippocampus, and does not have a precise anatomical definition since it is usually defined functionally; thus varying slightly between individuals and tasks at hand. It is the first region discovered to be scene-selective, as it responds strongly to stimuli with some sort of a spatial layout indicating a 3-dimensional space, compared to images of objects, faces, or scenes with disrupted spatial layouts (e.g. scrambled or noisy) [7].

Initial work on PPA including lesion studies demonstrated while the region is remarkably sensitive to spatial and categorical properties, as well as the initial learning of scenes and distinguishing landmarks, it may not be critical for processes related to navigation and recall from memory, such as landmark specific identity, reconstruction of places from memory, or different navigation systems [2, 8], implying the existence of a larger network of scene processing and navigation, with PPA being a part of it [3, 9].

Further studies demonstrated that PPA activation patterns differ between openness and closedness of a scene (spatial scale) [10], various scene categories [11, 12], and novelty and changes in viewpoint [13], and show a bias for the upper visual field where we usually find category-related information [14]; but not affected by tasks regarding route planning, navigation, or differences in the navigational ability of participants [15]. In addition, while many of these differences in activity patterns could partly be explained by variations in image statistics, PPA is thought to be involved in the higher-level understanding of scenes to some degree [16].

All things considered, PPA seems to be involved mainly in the processing of overall spatial properties (wholes) and the *gist*, that is, an initial summary of a scene, which are necessary for the recognition and categorization of scenes [17]; while less directly serving navigation or recall of familiar scenes and properties [18].

1.2.2 Retrosplenial Cortex/Medial Place Area

The retrosplenial cortex (RSC), or as it is recently referred to as the medial place area (MPA), lies within the posterior cingulate region encompassing Brodmann's 29 and 30. It is a region that is not only known for its scene-selectivity, but also for its roles in processes such as learning, navigation, and episodic memory [19]. Damage to the region causes problems in learning new routes and navigating previously known environments and is also considered to be a contributing factor to Alzheimer's disease, further indicating the role of this region in both learning and memory [19, 20]. It is also a component of the default mode network (DMN), an intrinsic brain activity network that is involved in passive states such as mind wandering or thinking of the past and the future, when not focused on the outside world or a task [21]

Activation patterns of RSC are modulated by changes in various properties of scenes and scene content; such as distance, orientation, and familiarity; representing changes in heading direction, both egocentric (in relation to self) and allocentric (object to object, like landmarks) distance, and landmark identity [22, 23], and is overall associated with spatial memory and deliberate, complex navigation making use of various variables [6, 18, 24, 25].

While other scene-selective regions are not prominent in memory-related processes, RSC is involved in processes such as mentally constructing scenes or map-based navigation that require considering places we are not currently situated within, either by prediction or retrieval from memory [26, 27]. RSC activation patterns do not represent category information as reliably as PPA [12], and the region does not show a visual field bias unlike PPA and OPA [14].

RSC's roles in a wide range of processes and its connections with many brain areas lead to it being considered a "hub", an association center responsible for integrating various types of spatial information and making predictions and plans by comparing the input to memory, regarding the broader environment [28], across perspective shifts and reference frames, boundaries, and landmarks [29, 30]. All these findings regarding RSC imply that its involvement in scene processing is intertwined with spatial memory to create a broader understanding of the environment, by bringing together various types of spatial information from both past and present experience, which are all necessary for successful route planning and map-based navigation.

1.2.3 Occipital Place Area

The occipital place area (OPA) is another scene-selective region located near the transverse occipital sulcus (TOS). It is associated with more automatic and lower-level processes regarding scenes, with its connections to PPA and RSC possibly implying it may be an information source for these regions that are partly associated with higher-level processes that require a deeper understanding of a scene and involving semantics, learning, and memory [31].

OPA is proposed to be central to visually guided navigation that concerns the immediate space visible to the eye, that do not require complex planning and retrieval of information from memory [32]. In fact, OPA activity is affected by changes in egocentric distance, first-person perspective (FPP) motion, direction, obstacles, and borders of a scene (e.g. walls, grounds, ceilings) [18, 33, 34], which are all important for action in the immediate environment; but unlike RSC, it is not significantly affected by changes in variables necessary for spatial learning or navigational planning regarding out-of-sight environments (map-based navigation) such as landmark identity, different reference frames, allocentric distance, location, or navigational complexity [6]. OPA also shows a lower visual field bias, where the ground for immediate action is usually located [14], further supporting its proposed function in immediate navigation.

TMS stimulation to OPA impairs navigation when the goal is described in relation to a wall (a border) [35], and also affects categorization accuracy [31]. However, other studies using categorization tasks suggest that OPA activation patterns do not represent category information as reliably as PPA [11, 12], which may be due to differences in border and obstacle content across scene categories that OPA is sensitive to [5].

These findings imply OPA's main role to be automatically and efficiently processing scene content based on visual features to support immediate action, and providing some information to other scene regions for further scene-processing without partaking in them itself.

1.3 Stimuli and Tasks in the Literature

As we mentioned in the previous sections, scene perception can be applied to any human activity and cognitive process that takes place within the context of a scene, with various stimulus content and tasks. We've also referred to studies from such topics to describe the different functions of scene-selective regions. To stay within the scope of this study, from this section on we will mainly focus on past behavioral and fMRI studies regarding the visual and behavioral factors that impact scene perception; such as semantic and visual properties of the scene stimuli and behavioral tasks given to participants to explore their impact.

In early scene research, and even to this day to some extent, tasks were either very limited or practically non-existent since the main goal was to examine how scene regions were responding to various types and features of scene stimuli. Therefore, the research question was addressed mainly by using different stimuli, primarily identified under different categories be it semantically or visually defined. Consequentially, the behavioral component in the majority of the field has been categorization tasks as well. Common categories employed in these studies include indoors vs outdoors [36, 37], natural vs urban or manmade [38, 39], various outdoor categories [40–42], and also distinctions that depend on various higher and lower level properties such as scale, openness, low vs high frequency, or color [43–46], and categories that are specific to task and research question such as navigational affordance level or familiarity of environments [27, 47, 48]. The study of such categories and stimulus features helped understand behavioral mechanisms of scene perception and define both similar and distinct functional roles of scene regions, such as variations in category sensitivity, semantic processing, and the impact of memory. However, the stimuli used were often nice, professional photos of environments, as defined by Epstein et al. “holiday snapshot perception” [5] or, on the contrary, very well-controlled images stripped of their various visual properties in order to study very specific representations regarding singular properties of scenes [49]; neither of which reflecting the actual real-life scene perception. Moreover, the way the scene categories were defined in these studies were often lacking a methodological approach, instead making distinctions based on one aspect of a scene (such as natural vs man-made) to either simplify the study of category sensitivity or just to give the participants a task while they investigate some other features regarding those scenes. Finally, the scene stimuli we come across in the majority of the literature belong to outdoor categories and nature, while the architectural indoors, where we spend most of our time (80-90% of our daily lives [50, 51]) are largely overlooked. The limited research that consists of such built environments as stimuli usually focuses on other cognitive processes such as navigation or aesthetics, rather than examining the perception of indoors and indoor categories specifically.

Other than the categorization tasks that complemented the stimulus focus of scene research mentioned above, what we often see are various n-back repetition detection tasks or similar that aim to keep the participant focused on what is displayed on the screen [52], rather than incorporating a behavioral aspect about the scenes. Although this may not be the case for scene research focusing on navigation, attention or memory that naturally require specific tasks, most research includes a task versus a rest or a localizer session at most. It has been pointed out several times before that incorporating ecologically valid stimuli and behavioral goals is necessary for a deeper understanding of scene perception [5, 16, 49], however, such work is still rare (recent examples, [53, 54]).

Therefore, to gain a complete understanding of scene perception in the human brain, more ecologically valid stimuli and tasks need to be integrated into experiments. To define such tasks one can be influenced by other disciplines that study environments, such as environmental psychology and neuroarchitecture, where we can approach a scene from various aspects; sensorimotor experience (approach, exploration, navigation), semantic associations (content, meaning), or emotional value (comfort, hominess, etc) to name a few [55]. While studying a particular level of features or goals and stripping off every other aspect of scenes and our behaviors regarding them is necessary to define finer, more sensitive underlying processes, it does not allow a holistic understanding of what it means to perceive and act within such complex, multi-faceted spaces that we spend our whole lives in.

1.4 The Present Study

In this present study, we aim to address the gaps mentioned so far from several aspects. First, this study focuses on how we perceive scenes from built environments, which have been largely overlooked in the literature. Second, in categorizing built environments, we adapt a principled approach from the architecture literature, as it is the primary field in designing, building, and studying these environments. Third, instead of irrelevant attention maintenance tasks, we use multiple behavioral tasks to understand how the behavioral goals of the observer shape scene perception in these environments. One of our tasks is a categorization task, which is commonly utilized in the literature to both keep the participant focused and investigate the high-level processes that it takes to understand an environment from different aspects. The other is an approach-avoidance task, since after perceiving and understanding a scene, one of the first actions that determine our future interaction or lack thereof with a scene is to either enter it or not. Approach-avoidance decisions are suggested to constitute a part of the initial processing of scenes that can be observed behaviorally [55], and we adapted this task to measure primary brain responses related to acting within scenes.

Further, we use a large stimulus set comprising ordinary-looking environments and utilize both traditional univariate and more sophisticated MVPA analysis techniques such as decoding and representational similarity analysis (RSA) to extensively inspect our research questions, at whole-brain and ROI levels.

Finally, we discuss our approach and findings within scene perception literature, as well as its possible implications for interdisciplinary research.

Research questions:

- Are brain activity patterns to built environments modulated by the behavioral goals of the perceiver?
- If so, how do these modulations differ across the brain, and the three scene-selective regions (PPA, RSC, OPA)?

Chapter 2

Methods

2.1 Participants

28 volunteers participated in this fMRI experiment. After data quality checks explained in section 2.8.1, 5 of them were removed from the analyses. Thus, the final sample comprised 23 participants (12 males/11 females, ages 18-31, M=23.9, SD=3.3). All participants had normal or corrected vision, reported not having any neurological disorders, and not using any such medication. The study was approved by the Human Research Ethics Committee of İhsan Doğramacı Bilkent University. Each participant filled out a prescreening form and gave written consent prior to the experiment. After the experiment, they were debriefed upon request and received course credits and/or 100 TL as compensation for their time.

2.2 Stimuli and Apparatus

Stimulus categories were defined based on Froyen's Universal Design; Users-Built Environments Model, which evaluates built environments from various perspectives for an in-depth classification [56]. This model was chosen because it focuses on universal, common properties of environments; also, it does not reduce these spaces to one aspect in order to categorize them, as has been the case in most previous scene research. This model, as shown in Figure 2.1 has two main classes, one is users, and the other is built environments. The user class is divided into two other dimensions; various needs and impairments any user may have, and activities one may perform in a given environment. The built environment class is further divided in two as well, with one dimension being various aspects affecting the physical and mental experience of users such as lighting, thermal conditions, aesthetics, and so on. The second dimension *elements* divides built environments into concrete sections based on their general purposes.

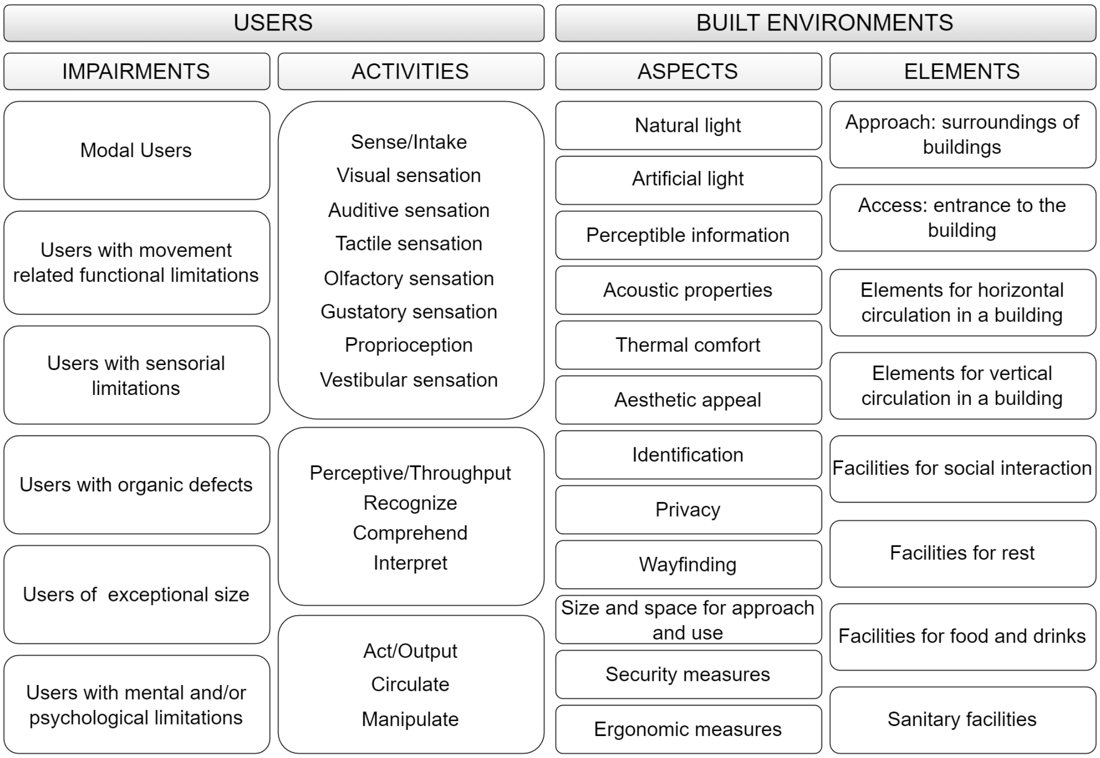

Figure 2.1: **Universal design Users-Built Environments model.** Proposed by Froyen, reproduced with permission [56].

Considering the objectives of this study, we decided to incorporate only the *elements* dimension of built environments. These categories were common to all public environments and were less personal; thus, they could be distinguished correctly by anyone. For participants to be able to learn these categories easily, we simplified them by grouping relevant categories together. As a result, we had two main categories based on the main types of action these areas afford. One was architectural elements, which contained areas that allow our access to and circulation within a building, mainly serving locomotion. The other was functional facilities, which contained areas serving basic needs that are common to every building; restrooms, eating areas with tables and chairs, and seating areas such as lobbies or waiting rooms; comprising rather stationary activities.

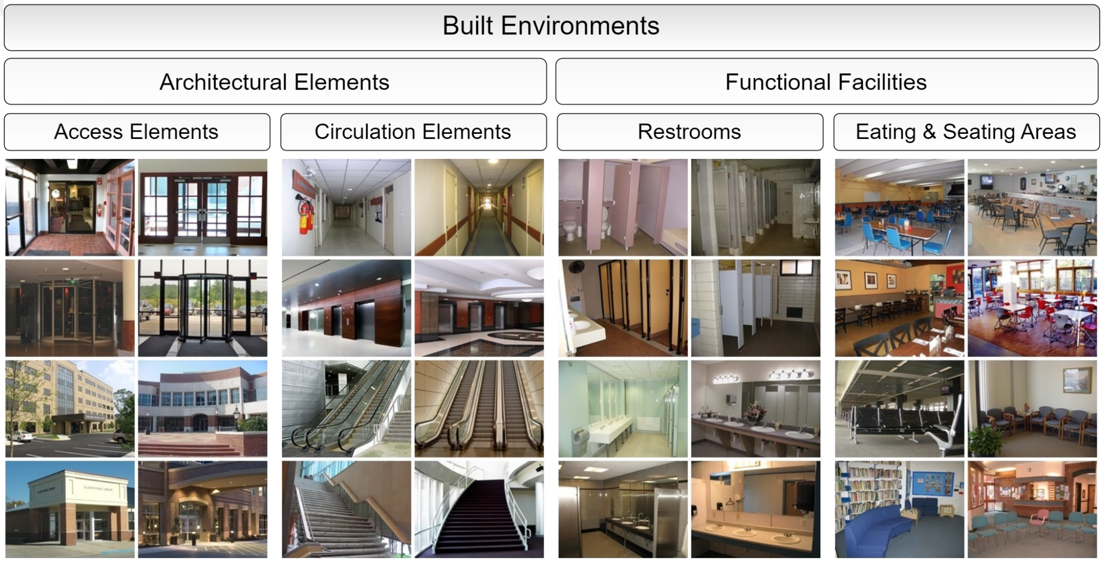

Figure 2.2: **Our simplified categories and the corresponding stimuli**

The final set of experimental stimuli consisted of 32 different images chosen from the Scene Understanding (SUN) database [57, 58]. There were 8 images of access elements to buildings (4 entrances, 4 exit points), 8 images of circulation elements (2 stairs, 2 escalators, 2 corridors, and 2 elevators), 8 images of sanitary facilities (4 bathroom cabins, 4 sink areas), and 8 images of seating areas (4 eating areas, 4 seating areas). Stimuli were presented on the screen with a 600x450 resolution. To keep the stimuli looking similar to real-life conditions, the visual properties of images were not manipulated to be equal, but this variation was instead addressed during analyses. Simplified categories and the corresponding stimuli used in the experiment can be seen in Figure 2.2.

2.3 Behavioral Tasks

Participants performed 2 different tasks during the experiment. One was a categorization task, where they responded by indicating which of the two main categories the presented stimuli belongs to. Since our categorization method was not reduced to a single feature of a scene and required considering different movements and actions a scene affords, along with understanding its semantic associations, our aim in choosing this task was to engage participants with various high-level processes required to wholly comprehend a scene.

The other was an approach-avoidance task, where they were simply asked to indicate whether they would like to enter the presented environment. Here we address our task as an "approach-avoidance task", however, it is important to note that it does not precisely represent the nature of such tasks found in the neuroscience literature. These types of tasks often involve distinctly separated stimuli based on either an apparent reward/punishment dynamic or a positive/negative valence to be interpreted by the observer [59]. In our case, it is more suitable to think of this task as an "enter-or-not" or a "go-no-go" decision to be made subjectively by the participants, since we neither chose our stimuli based on valence nor were interested in how the content is perceived emotionally. Rather, we aim to observe how a very first decision about acting in an environment is made, that is, to enter or not, based on an initial perception. Previous research in neuroarchitecture literature shows that approach-avoidance decisions are not completely explained by beauty or otherwise valence-based responses and that approach-avoidance tasks can measure initial sensorimotor processing regarding and environment [55]. Our instructions were also directed towards this idea, as we asked participants just to indicate their subjective, initial opinion on whether they want to be in the displayed environment or not, and emphasized that we do not expect them to answer a certain way or be consistent towards the same stimuli across runs. Therefore, this task is not analysed or interpreted similar to the classical approach-avoidance tasks, and is more proper to consider it to be unique to the aims of this study.

2.4 Experimental Design

The experimental design for the main experimental session is shown in Figure 2.3 and was implemented via a custom code written using Psychtoolbox-3 [60–62], working under MATLAB (The Mathworks Inc., Natick, MA). The experiment consisted of 8 runs. Each run consisted of 2 behavioral tasks as separate blocks within the run, counterbalanced across runs (ABBABAAB). Task blocks contained 32 trials (one trial for each stimulus) in random order. Each block within a run started with a 10-second instruction screen indicating which button corresponds to what response, and the trials followed. Trials began with a 2000ms of stimuli presentation, followed by a 2000ms response period, and ended with a randomized variable inter-stimulus interval (ISI) that ranged from 3000ms to 4000ms (mean=3500ms). At the end of each block, there was a 10-second rest period. A fixation cross was presented at the center of the screen at all times, which turned white only during the response period but was otherwise black.

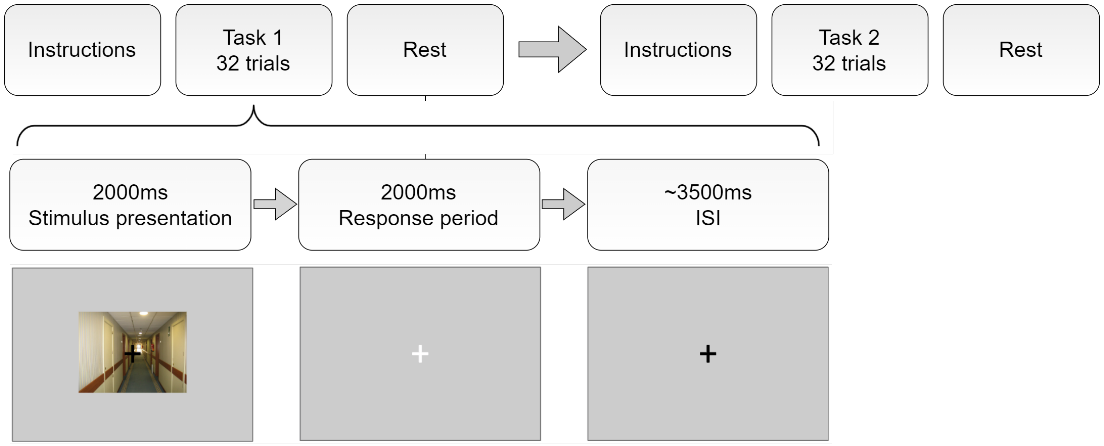

Figure 2.3: **The outline of the experimental procedure for one run.**

Participants were informed of the scene categories and the tasks they will perform. The architectural elements category was described as elements of buildings that help us access and circulate within a building as in moving from one place to another, and the functional facilities category was described as areas that serve basic human needs and comprise stationary activities. After learning the tasks, they completed a shorter version of the experiment on a laptop before the scans to ensure they understood the categories and the response procedure. Participants were asked to focus on the fixation throughout the experiment. The responses were collected using a fiber optic response box, with the keys corresponding to different answers based on the task.

2.5 Functional Localizer

We also conducted a short localizer session with the same participant group to define ROIs while avoiding double-dipping. 2 of them did not attend this session, and 5 participants who were removed from the main experiment were also removed from this one. Therefore, the final localizer sample included 21 participants (11 males/10 females, ages 18-31, M=23.7, SD=3.25). This experiment was adapted to our set-up by customizing the code made available by another study demonstrating its effectiveness across various age groups [63]. This experiment consisted of 4 runs, where participants viewed blocks of images rapidly presented on the screen with occasional repetitions, and performed a one-back repetition task. Blocks were either rectangles in shades of gray, scenes, or objects. The procedure and the randomization of blocks were the same as in the original study.

2.6 Data Acquisition

MRI data was collected using a 3T Siemens Trio scanner (Magnetom Trio, Siemens AG, Erlangen, Germany) with a 32-channel head coil, at the National Magnetic Resonance Research Center (UMRAM), İhsan Doğramacı Bilkent University. Participants viewed visual stimuli presented on an MRI-safe LCD screen (1920x1080px, 125x70cm, vertical refresh rate=60Hz, TROYKA MED, İstanbul) through a mirror mounted on the head coil with a total view distance of 168cm. The experiment consisted of 2 sessions for each participant. Both sessions started with a standard procedure, a short localizer scan to check if the head is positioned correctly, followed by a T1-weighted structural scan. The main experimental session further included 8 functional runs each lasting about 9 minutes. The functional localizer session included 4 functional runs each lasting 3 and a half minutes. The high resolution T1-weighted structural images were obtained with a standard protocol (TR=2600ms, TE=2.92ms, flip angle=12°, FoV read=256mm, FoV phase=87.5%, 176 slices, voxel size=1x1x1mm^3). During the functional runs, 263 functional volumes (104 for the localizer) were obtained using gradient-echo planar imaging (TR=2000ms, TE=22ms, flip angle=90°, 64x64 matric, FoV read=192mm, 43 slices with a thickness of 2.5mm, voxel size=3x3x2.5mm^3).

2.7 Behavioral Data Analysis

The accuracy of each participant for the categorization task was calculated to check if they could distinguish between categories. One participant who performed poorly was removed from further analyses. Reaction times were compared across tasks by performing a paired t-test. Responses to the approach-avoidance task were not considered since there were no correct answers. The behavioral results of the localizer experiment were not analyzed since the n-back task was only meant to keep the participant focused.

2.8 FMRI Data Preprocessing and Statistical Analyses

2.8.1 Anatomical and Functional Preprocessing

All the fMRI data in this manuscript were analysed after preprocessing using *fMRIPrep* 21.0.1 [64, 65] (RRID:SCR_016216), which is based on *Nipype* 1.6.1 [66, 67] (RRID:SCR_002502). Following preprocessing details and references are automatically created by the pipeline. Based on the output of this procedure, we extracted motion information for each run of each participant; runs with spikes of motion≥1.5mm and total relative motion≥3mm were removed from further analysis. 5 participants who had less than 5 suitable runs and one participant with neurological issues discovered during the scans were removed from further analyses. As a result of this process, the final group included a total of 23 participants, 18 of them with complete data, one participant with 7, two with 6, and one with 5 remaining functional runs. The same preprocessing steps were also applied to the functional localizer data. Data from participants who were completely removed from the main experiment analyses were also removed from this one. Further, 2 participants did not complete the localizer session, which left 21 participants for the localizer experiment.

2.8.1.1 Anatomical Data Preprocessing

A total of 2 T1-weighted (T1w) images were found within the input BIDS dataset. All of them were corrected for intensity non-uniformity (INU) with `N4BiasFieldCorrection` [68], distributed with ANTs 2.3.3 (RRID:SCR_004757) [69]. The T1w-reference was then skull-stripped with a *Nipype* implementation of the `antsBrainExtraction.sh` workflow (from ANTs), using OASIS30ANTs as target template. Brain tissue segmentation of cerebrospinal fluid (CSF), white-matter (WM) and gray-matter (GM) was performed on the brain-extracted T1w using `fast` (FSL 6.0.5.1:57b01774, RRID:SCR_002823) [70]. A T1w-reference map was computed after registration of 2 T1w images (after INU-correction) using `mri_robust_template` (FreeSurfer 6.0.1) [71]. Brain surfaces were reconstructed using `recon-all` (FreeSurfer 6.0.1, RRID:SCR_001847) [72], and the brain mask estimated previously was refined with a custom variation of the method to reconcile ANTs-derived and FreeSurfer-derived segmentations of the cortical gray-matter of Mindboggle (RRID:SCR_002438) [73]. Volume-based spatial normalization to one standard space (MNI152NLin2009cAsym) was performed through nonlinear registration with `antsRegistration` (ANTs 2.3.3), using brain-extracted versions of both T1w reference and the T1w template. The following template was selected for spatial normalization: *ICBM 152 Nonlinear Asymmetrical template version 2009c* (RRID:SCR_008796; TemplateFlow ID:MNI152NLin2009cAsym) [74].

2.8.1.2 Functional Data Preprocessing

For each of the 8 BOLD runs (4 runs for the localizer) found per subject (across all tasks and sessions), the following preprocessing was performed. First, a reference volume and its skull-stripped version were generated using a custom methodology of *fMRIPrep*. Head-motion parameters with respect to the BOLD reference (transformation matrices, and six corresponding rotation and translation parameters) are estimated before any spatiotemporal filtering using `mcflirt` (FSL 6.0.5.1:57b01774) [75]. BOLD runs were slice-time corrected to 0.98s (0.5 of slice acquisition range 0s-1.96s) using `3dTshift` from AFNI (RRID:SCR_005927) [76]. The BOLD time-series (including slice-timing correction when applied) were resampled onto their original, native space by applying the transforms to correct for head-motion. These resampled BOLD time-series will be referred to as *preprocessed BOLD in original space*, or just *preprocessed BOLD*. The BOLD reference was then co-registered to the T1w reference using `bbregister` (FreeSurfer) which implements boundary-based registration [77]. Co-registration was configured with six degrees of freedom. Several confounding time-series were calculated based on the *preprocessed BOLD*: framewise displacement (FD), DVARS and three regionwise global signals. FD was computed using two formulations following Power (absolute sum of relative motions, [78]) and Jenkinson (relative root mean square displacement between affines, [75]). FD and DVARS are calculated for each functional run, both using their implementations in *Nipype* [following the definitions by 78]. The three global signals are extracted within the CSF, the WM, and the whole-brain masks. Additionally, a set of physiological regressors were extracted to allow for component-based noise correction (*CompCor* [79]). Principal components are estimated after high-pass filtering the *preprocessed BOLD* time-series (using a discrete cosine filter with 128s cut-off) for the two *CompCor* variants: temporal (tCompCor) and anatomical (aCompCor). tCompCor components are then calculated from the top 2% variable voxels within the brain mask. For aCompCor, three probabilistic masks (CSF, WM and combined CSF+WM) are generated in anatomical space. The implementation differs from that of Behzadi et al. in that instead of eroding the masks by 2 pixels on BOLD space, the aCompCor masks are subtracted a mask of pixels that likely contain a volume fraction of GM. This mask is obtained by dilating a GM mask extracted from the FreeSurfer's *aseg* segmentation, and it ensures components are not extracted from voxels containing a minimal fraction of GM. Finally, these masks are resampled into BOLD space and binarized by thresholding at 0.99 (as in the original implementation). Components are also calculated separately within the WM and CSF masks. For each CompCor decomposition, the k components with the largest singular values are retained, such that the retained components' time series are sufficient to explain 50 percent of variance across the nuisance mask (CSF, WM, combined, or temporal). The remaining components are dropped from consideration. The head-motion estimates calculated in the correction step were also placed within the corresponding confounds file. The confound time series derived from head motion estimates and global signals were expanded with the inclusion of temporal derivatives and quadratic terms for each [80]. Frames that exceeded a threshold of 0.5 mm FD or 1.5 standardised DVARS were annotated as motion outliers. The BOLD time-series were resampled into standard space, generating a *preprocessed BOLD run in MNI152NLin2009cAsym space*. First, a reference volume and its skull-stripped version were generated using a custom methodology of *fMRIPrep*. All resamplings can be performed with *a single interpolation step* by composing all the pertinent transformations (i.e. head-motion transform matrices, susceptibility distortion correction when available, and co-registrations to anatomical and output spaces). Gridded (volumetric) resamplings were performed using `antsApplyTransforms` (ANTs), configured with Lanczos interpolation to minimize the smoothing effects of other kernels [81]. Non-gridded (surface) resamplings were performed using `mri_vol2surf` (FreeSurfer).

2.8.2 Whole-Brain Analyses

2.8.2.1 Univariate Analysis

The same smoothing steps were followed as the functional localizer analyses. Using a design matrix of 18 regressors (8 experimental regressors (4 for categories under categorization task, 4 for categories under approach-avoidance task), 1 for rests, 1 for ISIs (fixation), 1 for instructions, 1 for responses, and 6 motion regressors; 3 for rotations, 3 for translations) general linear model (GLM) was calculated for each participant, within their individual brain masks created by the preprocessing procedure to avoid any remaining skull tissue interfering with analysis. Regressors were convolved using the default canonical hemodynamic response function under SPM12. Contrasts images of each participant were created for task and category comparisons.

Later, t-tests were performed as group-level analyses with default parameters in SPM, using the corresponding contrast images of each participant, including tasks > rest, categorization > approach-avoidance, and approach-avoidance > categorization contrasts.

2.8.2.2 Searchlight-Based Multivariate Pattern Analyses (MVPA)

Same GLM analyses were also performed on unsmoothed data for MVPA analyses. We used The Decoding Toolbox (TDT - version 3.999F, [82]) to train and test classifiers to discriminate between the two tasks, at the whole-brain level. A linear support vector machine (LibSVM) [83] was implemented with a fixed cost parameter of c=1. Each participant's runwise beta images from the GLM analyses were used to train the classifiers employing a leave-one-run-out procedure, where at each step, the training data was all runs but one for each participant, and the remaining run was used to test the classifier. Classifier was trained in this fashion repeatedly to test for each run while training with the rest (k=8 for 18, k=7 for 1, k=6 for 3, and k=5 for 1 participant). We used the searchlight approach, moving a sphere with a 4mm radius [84] within each subject's brain mask. As a result, each participant's accuracy minus chance brain images were created and smoothed using a full width at half maximum (FWHM)=6mm kernel to increase spatial correspondence across the group and put through a one-sample t-test for the group-level analysis.

This procedure was performed over all subjects twice, once classifying for the tasks (labels: 1,-1), and once classifying for category independent of the task (labels: 1,2,3,4). Testing and training designs for a typical 8-run application for both conditions are shown in Supplementary Figures A.2 and A.3

2.8.3 Region of Interest (ROI) Analyses

2.8.3.1 Functional Localizer Analysis and Definition of ROIs

Functional scans were smoothed with a full width at half maximum (FWHM)=6mm kernel on top of preprocessing. Both smoothing and 1^{st} level as well as group-level analyses were conducted using the Statistical Parametric Mapping software package (SPM12, Wellcome Trust Centre for Neuroimaging, University College London, UK) implemented under MATLAB (The Mathworks Inc., Natick, MA). Using a design matrix of 11 regressors (scenes, objects, fixation, rest, instructions, and 6 motion regressors; 3 for rotations, 3 for translations) general linear model (GLM) was calculated for each participant with the same parameters as the main experiment. Contrast images of each participant were created for the scenes > objects contrast. Using these contrasts, a group-level analysis (one-sample t-test) was performed using default SPM parameters.

To avoid overlapping regions and guide deciding the extent of these regions, we followed the parcellation method by Julian et al [85]. They conducted a longer localizer experiment on a large group of participants for various categories and used thresholded activation maps of each participant to create parcels that indicate the maximum probable area across individuals for that region of interest.

We used these parcels as a rough guide on where to find our ROIs, and using MarsBar toolbox [86] working under SPM12, defined the strongest responding 50-voxel clusters around the region for each ROI by adjusting the threshold.

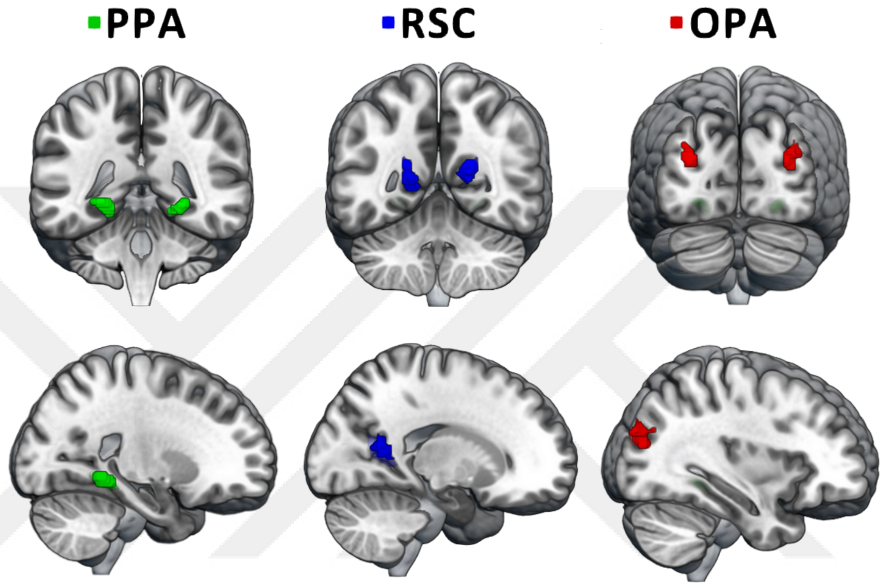

Figure 2.4: **Final ROI masks based on the group-level analysis**

The resulting 50-voxel images were then combined with their counterparts using MarsBar, resulting in 3 bilateral ROI masks containing 100 voxels. Visualized ROI masks are shown in Figure 2.4. Final ROI peak coordinates were similar to the findings in the literature, shown in Table 2.1.

Table 2.1: **Coordinates and peak thresholds of the defined ROIs.**

Region of interest	Left hemisphere			Right hemisphere		
	Cluster threshold	Peak threshold	Peak coordinates	Cluster threshold	Peak threshold	Peak coordinates
PPA	T=9	T=15.42 T=9.41	-24 -48 -6 -22 -36 -14	T=9.2	T= 19.71	26 -46 -6
RSC	T=6.5	T=11.27 T=8.43 T=5.43	-18 -58 9 -16 -48 4 -6 -42 2	T=8.5	T=14.11	20 -54 14
OPA	T=3.95	T=6.57 T=5.05	-30 -84 22 -34 -82 32	T=6.06	T=8.25 T=8.07 T=6.72	32 -78 19 32 -84 26 38 -78 26

2.8.3.2 Representational Similarity Analysis (RSA)

Representational Similarity Analysis (RSA) is a method for examining the similarity of neural activity patterns across different conditions or stimuli [87]. By examining the changes in patterns of responses simultaneously across the brain or selected regions, it helps us learn more about the underlying representations and how the information is processed compared to univariate analyses that only determine overall activation differences. Representational dissimilarity matrices (RDMs) defined in this method contain dissimilarity values for each pair of conditions, at the cross-sections of rows and columns representing each condition in both axes. As a result, there is an n x n matrix (n=number of conditions) that has color-coded cells for each value, naturally creating a solid diagonal for the points each condition is paired with itself. The resulting matrix is then compared to planned models that are either hypothesized or based on possible confounds such as visual, semantic, or task-based models.

We performed a model-based RSA at both whole-brain and ROI-level to investigate the task effect on the modulation of neural activity to our built environment categories. We modified the scripts that are included in the RSA Toolbox [88] to fit our experiment. A separate set of GLM analyses with the same parameters were performed on the unsmoothed fMRI data for the RSA; only in this case, the design matrix consisted of 64 instead of 8 experimental regressors (32 stimuli x 2 tasks). Contrast images for all 64 of them were created compared to rest. Resulting thresholded SPM images (spmT's) were used as input to the toolbox.

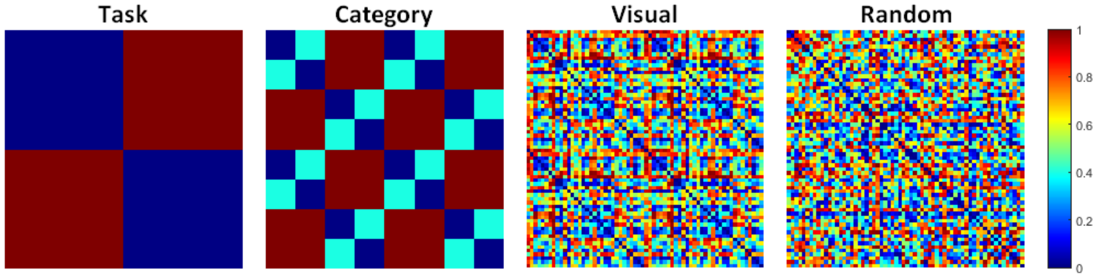

Figure 2.5: **Models created for RSA**

For every ROI, averaged RDMs were created across 23 subjects and compared to the models, performing a one-sided Wilcoxon signed-rank random-effects test (via Kendall's τ). The upper and lower bounds of the noise ceiling were calculated by estimating a hypothetical model with maximum average correlation to the reference RDM, again via Kendall's τ. Pairwise correlations of all the RDMs (every ROI and model) were then compared by calculating Spearman's ρ.

For model comparisons, four alternative models were created (Figure 2.5). The first was a task model with higher similarity values for the same task, to test if the behavioral goals of the subjects affect the neural patterns in our ROIs. The second was a category level with higher similarity values for items of the same subcategory, and again high values for same main category regardless of the task; to assess if there were any impact of scene categories we chose on neural activation patterns. We added this model since these scene-selective regions have been reported to have different patterns of activation towards scene categories, as we described in the introduction section. The third model was a visual model in order to test if there were any correlation between the visual similarities of images and the neural activation patterns, created by calculating the mean correlation between each image pair on three color dimensions (RGB), and then transforming it to a correlation distance value by subtracting the value from 1. The final model was a random control model. For visualization and coherence purposes, matrix values of both models and actual brain results were rank transformed into [0,1] and color-coded accordingly.

Chapter 3

Results

3.1 Behavioral Results

3.1.1 Accuracy

For the categorization task, all participants included in the final analyses (N=23) performed well, indicating that the categories were understood. Mean accuracy was 96.98% (84-100%, SD=3.8).

3.1.2 Reaction Times

To investigate differences across tasks in reaction times, we ran a paired samples t-test (Figure 3.1). Participants responded faster during the categorization task (p<0.001), though with a very small effect size (Cohen's d=0.103), which implies that the two tasks do not necessarily differ a considerable amount in terms of the attention paid by participants.

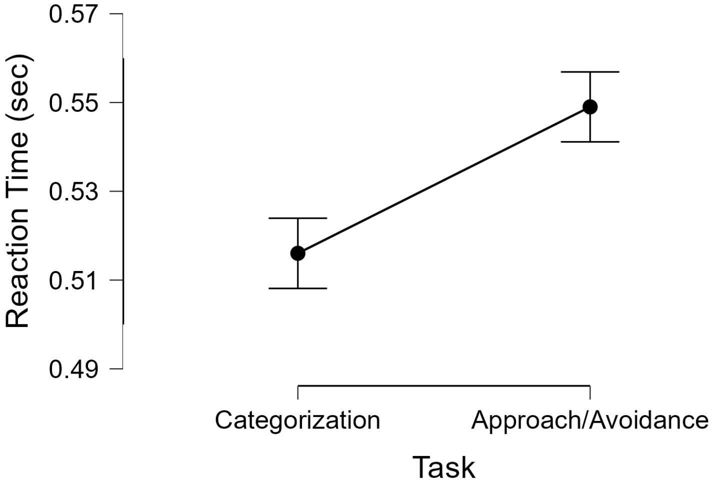

Figure 3.1: **Reaction times across tasks.** Results were significant at $p<0.001$, Cohen's d (effect size) = 0.103.

3.2 FMRI Results

Activation maps shown in Figures 3.2, 3.3, 3.4, 3.5, and A.1 were visualized using Workbench v1.5 [89]. Supplementary Figure A.1 displays all tasks > rest contrast for reference.

3.2.1 Univariate Results and Activation Maps

3.2.1.1 Categorization > Approach-Avoidance

For this contrast, only 3 small clusters were observed at $p<0.05$, family-wise error rate (FWE) corrected. These were, a 2-voxel cluster at the right supramarginal gyrus (peak: 66, -36, 24; T=7.58), a 3-voxel cluster at the right middle cingulate (peak: 12, -18, 39; T=7.30), and a voxel at the left postcentral gyrus (peak: -48, -30, 62; T=6.68). The rest of the results reported below were at a threshold of $p<0.001$ (uncorrected, extent=10 voxels).

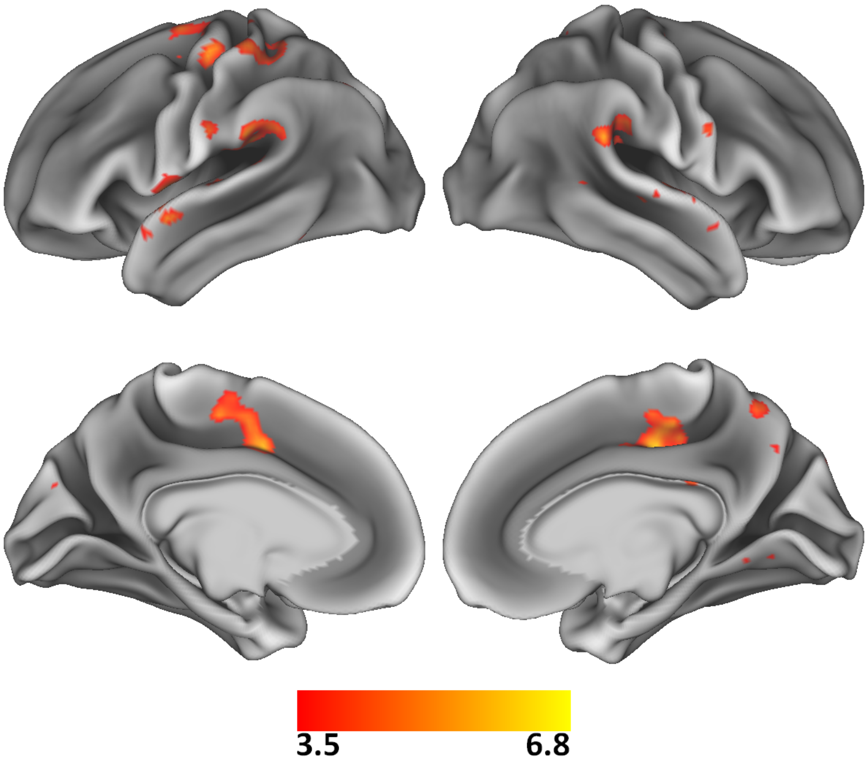

Figure 3.2: **Activation map of the categorization > approach-avoidance contrast.** The results were at p<0.001, uncorrected.

Shown in Figure 3.2, this contrast mainly yielded bilateral activation in parietal regions such as the supramarginal gyrus (SMG) and the precuneus, postcentral and precentral gyri making up the primary somatosensory cortex (S1). In the left hemisphere, there was a large cluster peaking at the supplementary motor area (SMA) extending into the superior temporal gyrus (STG). There were also clusters at the temporal regions including the STG and middle temporal gyrus (MTG) and the occipital regions, and the dorsal and ventral striatum including the caudate, putamen, and the nucleus accumbens. All the peaks, peak T-values, and the regions the clusters extend into are listed in Table 3.1, and are consistent with the scene perception literature.[90]

Table 3.1: **Peak regions for the categorization > approach-avoidance contrast.** Results were at $p<0.001$, uncorrected. Extent threshold=10 voxels.

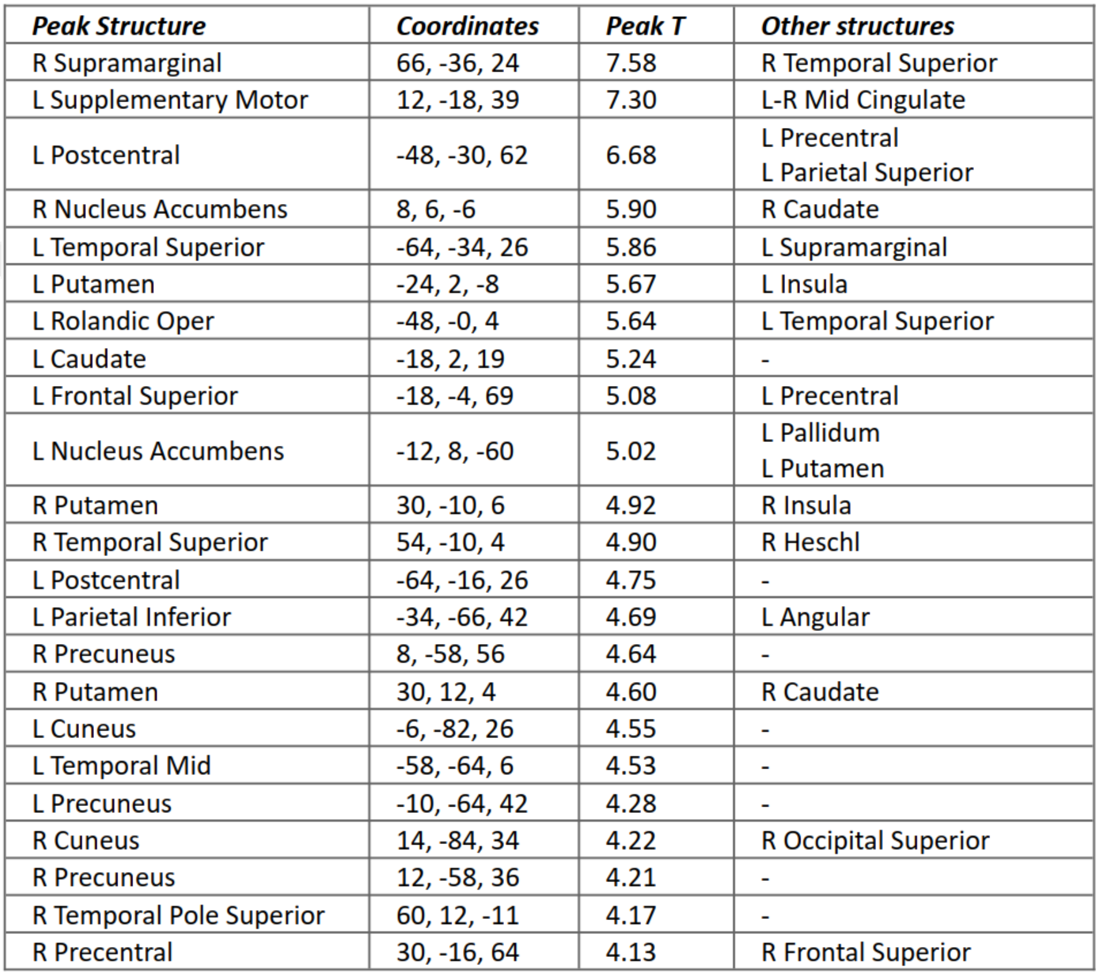

Peak Structure	***Coordinates***	***Peak T***	***Other structures***
R Supramarginal	66, -36, 24	7.58	R Temporal Superior
L Supplementary Motor	12, -18, 39	7.30	L-R Mid Cingulate
L Postcentral	-48, -30, 62	6.68	L Precentral L Parietal Superior
R Nucleus Accumbens	8, 6, -6	5.90	R Caudate
L Temporal Superior	-64, -34, 26	5.86	L Supramarginal
L Putamen	-24, 2, -8	5.67	L Insula
L Rolandic Oper	-48, -0, 4	5.64	L Temporal Superior
L Caudate	-18, 2, 19	5.24	-
L Frontal Superior	-18, -4, 69	5.08	L Precentral
L Nucleus Accumbens	-12, 8, -60	5.02	L Pallidum L Putamen
R Putamen	30, -10, 6	4.92	R Insula
R Temporal Superior	54, -10, 4	4.90	R Heschl
L Postcentral	-64, -16, 26	4.75	-
L Parietal Inferior	-34, -66, 42	4.69	L Angular
R Precuneus	8, -58, 56	4.64	-
R Putamen	30, 12, 4	4.60	R Caudate
L Cuneus	-6, -82, 26	4.55	-
L Temporal Mid	-58, -64, 6	4.53	-
L Precuneus	-10, -64, 42	4.28	-
R Cuneus	14, -84, 34	4.22	R Occipital Superior
R Precuneus	12, -58, 36	4.21	-
R Temporal Pole Superior	60, 12, -11	4.17	-
R Precentral	30, -16, 64	4.13	R Frontal Superior

3.2.1.2 Approach-Avoidance > Categorization

For this contrast, only 2 peaks were observed at $p<0.05$, FWE-corrected. One of these was at the left supplementary motor area (peak: -6, 20, 46; T=6.83), and the other was at the right cuneus (peak: 20, -58, 19; T=6.59). The rest of the results reported below were at a threshold of $p<0.001$ (uncorrected, extent=10 voxels).

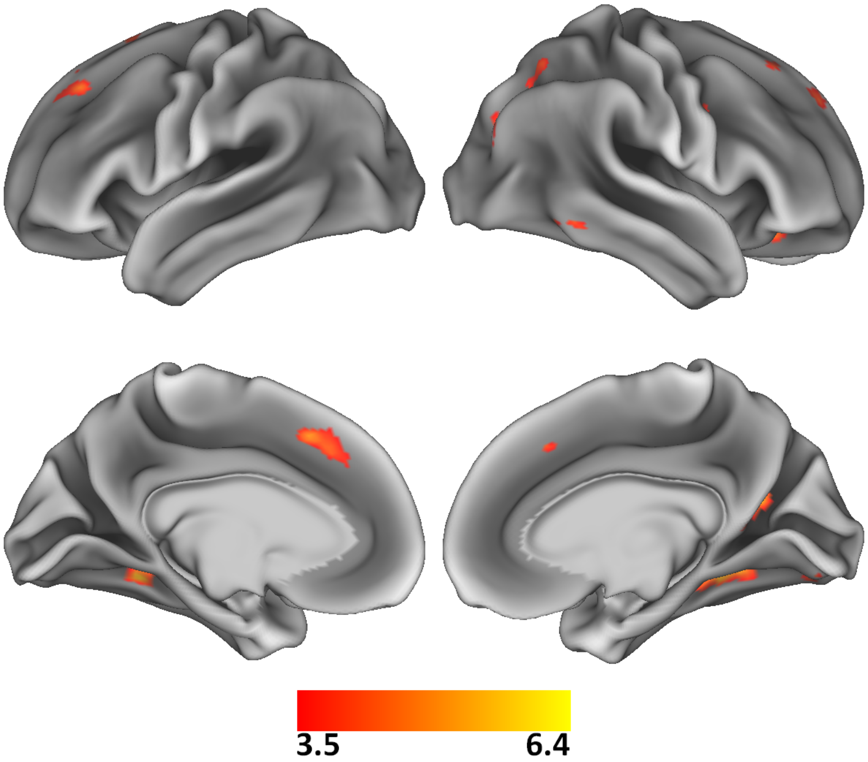

Figure 3.3: **Activation map of the approach-avoidance > categorization contrast.** The results were at $p<0.001$, uncorrected.

Shown in Figure 3.3, this contrast mainly yielded activation in category-selective regions bilaterally, including the lingual, parahippocampal, and fusiform gyri, which make up parts of the PPA and RSC. We also observed activation in superior occipital areas, partly within the region we often observe the OPA. There were also clusters in other visual areas such as the cuneus and the calcarine sulcus, in parietal regions including the precuneus, and superior frontal areas. All the peaks, peak T-values, and the regions the clusters extend into are listed in Table 3.2, and the indicated regions have been reported previously regarding scene processing and approach-avoidance tasks [53, 91, 92].

Table 3.2: **Peak regions for the approach-avoidance > categorization contrast.** Results were at $p<0.001$, uncorrected. Extent threshold=10 voxels.

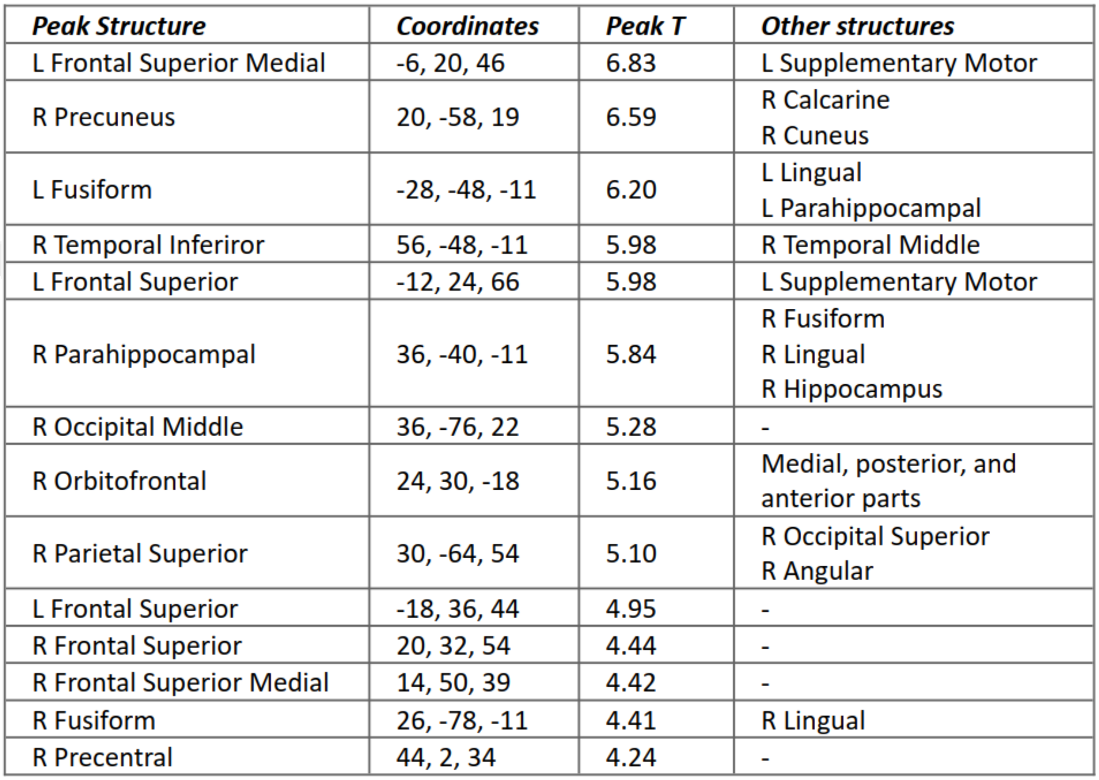

Peak Structure	***Coordinates***	***Peak T***	***Other structures***
L Frontal Superior Medial	-6, 20, 46	6.83	L Supplementary Motor
R Precuneus	20, -58, 19	6.59	R Calcarine R Cuneus
L Fusiform	-28, -48, -11	6.20	L Lingual L Parahippocampal
R Temporal Inferiror	56, -48, -11	5.98	R Temporal Middle
L Frontal Superior	-12, 24, 66	5.98	L Supplementary Motor
R Parahippocampal	36, -40, -11	5.84	R Fusiform R Lingual R Hippocampus
R Occipital Middle	36, -76, 22	5.28	-
R Orbitofrontal	24, 30, -18	5.16	Medial, posterior, and anterior parts
R Parietal Superior	30, -64, 54	5.10	R Occipital Superior R Angular
L Frontal Superior	-18, 36, 44	4.95	-
R Frontal Superior	20, 32, 54	4.44	-
R Frontal Superior Medial	14, 50, 39	4.42	-
R Fusiform	26, -78, -11	4.41	R Lingual
R Precentral	44, 2, 34	4.24	-

3.2.2 Searchlight-Based MVPA Results

Since what we can learn about brain activity patterns and how it is modulated by task is limited using univariate analysis techniques, multivariate pattern analyses were conducted to identify regions that could discriminate between task conditions and categories by conducting a one-sample t-test over participants' smoothed accuracy minus chance images.

3.2.2.1 Classification Results for Task

The results here are reported at p<0.001 (uncorrected) (Figure 3.4, listed peaks include clusters of at least 10 voxels since this is not a strict threshold 3.3. No voxels survived FWE correction.

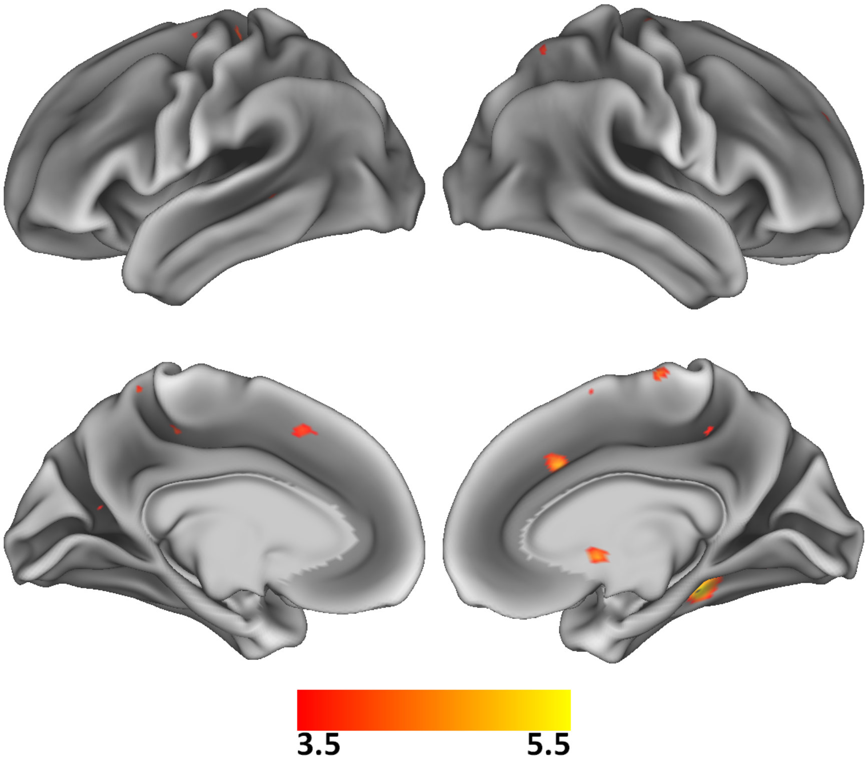

Figure 3.4: **Decoding regions for task classification.** The results were at p<0.001, uncorrected. Extent threshold=10 voxels.

We observed above-chance decoding performance at the regions that were previously found to have good decoding accuracy regarding scenes; right fusiform gyrus [93] extending into the parahippocampal gyrus [94]. Decoding performance was also significant at the left calcarine, right insula and middle cingulate gyrus, bilateral SMAs, and a portion of the left medial superior frontal area, which are also crucial for scene processing [95], although to the best of our knowledge, not particularly related to behavioral tasks.

Table 3.3: **Peaks with above-chance classification accuracy for task.** Results were at $p<0.001$, uncorrected. Extent threshold=10 voxels.

Peak Structure	***Coordinates***	***Peak T***	***Other structures***
R Fusiform	32, -36, -16	5.97	R Parahippocampal
L Calcarine	-22, -66, 16	5.64	-
R Cingulate Middle	8, 20, 34	4.93	-
R-L Supplementary Motor	-0, 8, 64	4.72	-
L Frontal Superior Medial	-6, 44, 36	4.35	-
R Supplementary Motor	8, 24, 64	4.26	R Frontal Superior Medial
R Insula	48, 12, -1	4.25	R Frontal Inferior Opercular

3.2.2.2 Classification Results for Scene Category

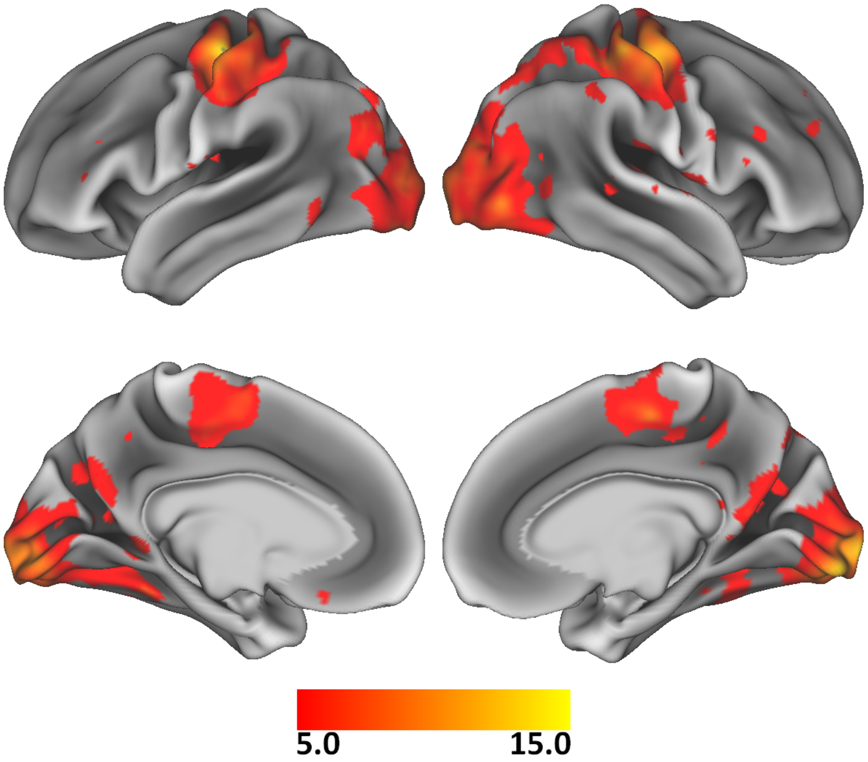

Figure 3.5: **Decoding regions for category classification.** The results were at $p<0.05$, FWE-corrected.

The results for category decoding performance independent of the task are reported at $p<0.05$ (FWE-corrected, extent=2 voxels) (Figure 3.5. At this threshold, all the clusters are listed in table 3.4.

The stimulus categories were decoded above chance in many regions. Most significant of these were bilateral clusters in regions encompassing the lingual gyrus and calcarine sulcus, precentral and postcentral gyri, as well as the SMAs. The classification accuracy was also significant in occipital regions, as well as some parts of the parietal and temporal cortex. These regions are all consistent with the literature, as they were reported to have good classification performance for category [94, 96, 97].

Table 3.4: **Peaks with above-chance classification accuracy for category.** Results were at $p<0.05$, FWE-corrected. All peak regions and regions the cluster extends into are listed. Extent threshold=2 voxels.

Peak Structure	***Coordinates***	***Peak T***	***Other structures***
R Lingual	8, -90, -11	15.35	L-R Calcarine
R Calcarine	14, -102, -1	14.94	R Occipital Superior R Cuneus
R Occipital Inferior	32, -84, -11	12.17	R Fusiform
L Precentral	-40, -22, 59	15.32	-
L Postcentral	-40, -28, 66	12.26	-
L Postcentral	-54, -16, 54	10.75	L Parietal Inferior
R Precentral	42, -24, 59	13.83	-
R Precentral	44, -16, 54	12.88	-
R Postcentral	32, -30, 52	12.54	-
R Occipital Inferior	48, -78, -4	10.12	R Occipital Middle
R Supplementary Motor	6, -16, 54	9.51	R Cingulate Middle
L Supplementary Motor	-0, -6, 64	8.35	R Supplementary Motor
L Fusiform	-24, -42, -18	8.73	L Cerebellum
L Occipital Middle	-36, -84, 26	8.57	L Angular
R Occipital Inferior	48, -72, -16	8.04	R Fusiform
L Supramarginal	-54, -22, 42	7.78	L Parietal Inferior
L Lingual	-10, -48, -1	7.10	L Cerebellum
R Occipital Superior	14, -96, 22	7.02	R Cuneus
R Occipital Middle	48, -78, 14	6.98	R Temporal Middle

3.2.3 RSA Results

Since whole-brain analyses do not give the whole picture considering the existence of category-sensitive regions, we examined the three scene-selective regions (PPA, RSC, OPA) by conducting an RSA. In this analysis, our aim was not to identify regions that show higher activation to certain conditions or have better classification accuracy but rather to examine the similarities and differences between activation patterns across conditions and ROIs.

Neural RDMs are shown in Figure 3.6-A, displaying dissimilarity values averaged across 23 participants. Figure 3.6-B shows the MDS plots (calculated by minimizing metric stress) of color-coded categories across tasks. MDS Shepard plots for ROI RDMs are shown in Supplementary Figure A.4.

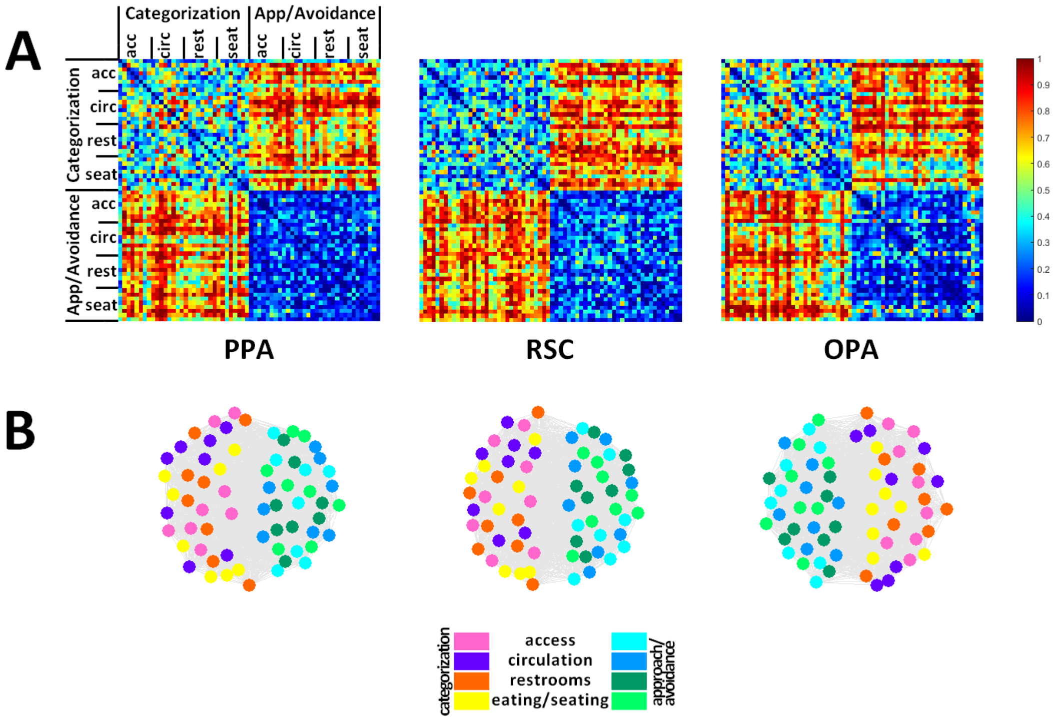

Figure 3.6: **A) Subject-averaged RDMs of 3 scene-selective regions.** Each dissimilarity matrix (64^2) is separately rank-transformed and scaled into [0,1].**B) MDS plots of conditions across tasks.** Differences in representations across ROIs for tasks and categories are demonstrated.

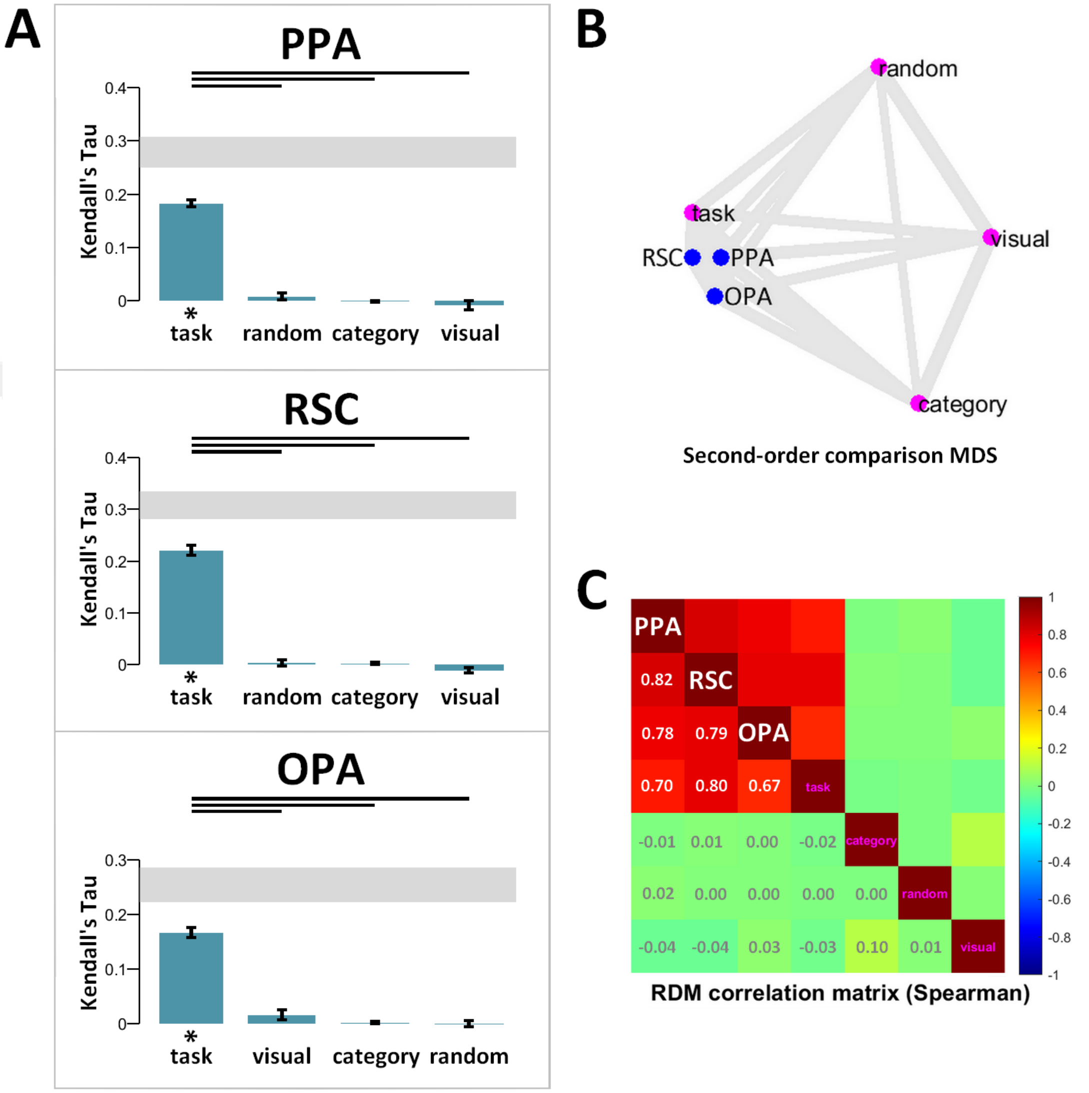

PPA						
0.82	RSC					
0.78	0.79	OPA				
0.70	0.80	0.67	task			
-0.01	0.01	0.00	-0.02	category		
0.02	0.00	0.00	0.00	0.00	random	
-0.04	-0.04	0.03	-0.03	0.10	0.01	visual

Figure 3.7: **A) Comparison of neural RDMs and model RDMs.** Kendall's τ was used to compare ROIs to models across 23 subjects. Gray bands over the graphs indicate the noise ceiling, black lines indicate significant differences between models, and (*) indicates similarities to the ROI at $p<0.01$. **B) Second-order comparison MDS.** Indicates the Spearman distance measure between the ROI and model RDMs. **C) RDM correlation matrix.** Indicating the Spearman correlations of ROI and model RDMs.

We compared these RDMs to our models described in the last chapter (section 2.8.5), performing a signed-rank random-effects test, corrected for multiple comparisons (FDR - False Discovery Rate), at a threshold of $p<0.01$ via computing their Kendall's τ. ROI vs Model comparisons are shown in Figure 3.7-A.

For all ROIs, only the Task model was significantly related to the neural RDM at hand (at $p<0.01$, FDR corrected). By the same criteria, Category, Visual, and Random models were significantly different from the task model, but not from one another.

To be specific, for the PPA, Kendall's τ values for the models were as follows: Task (0.182, p=0.000), Category (-0.002, p=0.82), Visual (-0.009, p=0.82), and Random (0.008, p=0.172). None of the models reached within the bounds of the noise ceiling (0.249, 0.308). For RSC, the results were similar. Kendall's τ values for neither Task (0.221, p=0.000), Category (0.003, p=0.172), Visual (-0.011, p=0.957), nor Random (0.003, p=0.251) models exceeded the lower bound of the noise ceiling (0.281, 0.334). For OPA, the same trend followed (Kendall's τ: Task (0.166, p=0.000), Category (0.000, p=0.4), Visual (0.015, p=0.106), Random (-0.001, p=0.577); the noise ceiling: (0.223, 0.286))

Second-level MDS plots are shown in Figure 3.7-B, spatially demonstrating the representational proximity of the 3 ROIs and the comparison models. The results of the pairwise comparisons of each RDM (both neural and model) are shown in Figure 3.7-C. Shepard plot for pairwise RDM comparison is shown in Supplementary Figure A.5.

Chapter 4

Discussion

In this thesis project, we presented an extensive examination of the impact of behavioral goals on the neural responses to scenes.

Our research question arose from recognizing the scarcity of diverse behavioral tasks and a principled approach to categorization within the scene perception literature regarding indoor environments. Acknowledging these gaps, our objective was to address them by incorporating relevant behavioral tasks and utilizing a categorization methodology inspired by relevant fields.

In order to examine the task effect at the whole-brain and ROI levels, multiple analysis techniques were employed including traditional univariate analyses and more elaborate multivariate analysis techniques such as decoding and RSA. Moreover, we also included additional analyses and comparison models to probe other possible patterns that may be informative.

As a result, we observed that while there was not a remarkable task effect discoverable by univariate analyses alone, multivariate techniques uncovered different effects of task and stimuli properties at the whole-brain and ROI-level. Various brain regions could classify scene categories, while the task impact affected the scene-selective regions.

In this final chapter, I will discuss the implications of our findings and their contribution to the literature and identify the limitations of this present study. I will also evaluate the possible directions for future research from an interdisciplinary perspective.

4.1 Univariate Analyses Do Not Give Us the Whole Picture

To examine the direct differences between brain activity levels while participants were engaged in two separate tasks, we conducted univariate analyses on two contrasts, categorization > approach-avoidance, and the vice-versa.

For the categorization > approach-avoidance contrast, there were only local peaks in three areas, the right supramarginal gyrus, the right middle cingulate gyrus, and the left postcentral gyrus.

Further, at a more liberal threshold, we observed activity in regions that have been associated with high-level processing regarding scenes such as parts of the inferior parietal lobule (SMG), MTG, STG, the precuneus, and the cingulate gyrus [90], and are often iterated in findings of navigation studies regarding visually guided action, reference frames, and localization as well [6, 98]. These regions have also been associated with memory, imagination, and linking various types of information and spatial representations of one's body [99, 100], and are high in scene category decoding performance [96]. Inferior and superior parietal regions, as well as various motor regions, have also been associated with the coding of the affordances of environments [101], and may imply a task difference regarding affordances since the categorization task was heavily based on types of actions and movements a place fundamentally affords. Independent of the scene literature, the activated regions constitute parts of several large-scale brain networks; mainly the ventral and dorsal attention networks, the central executive, and the sensorimotor network (SMN) [102, 103], expected in tasks that require semantic and visuospatial processing. However, it is important to emphasize these results are at an uncorrected threshold of $p<0.001$ and do not imply a definite task effect at the whole-brain level.

For the approach-avoidance > categorization contrast, there were only two local peaks, at the left supplementary motor area and the right cuneus.

At a less strict threshold, the activity observed mainly at the medial and superior frontal areas, the precuneus, and the parahippocampal region, has previously been associated with engaging egocentric reference frames, which means the observer evaluating the environment based on their own position [95]. This may imply that when the observers were asked to decide whether they would like to enter a scene, they evaluated the environment by referring to their own presence. Active regions also include those associated with spatial representations in general, such as inferior and middle temporal gyri, and middle occipital gyrus [95], with middle and lateral occipital regions that are also thought to have a role in processing the local elements of scenes [104]. The activity in the frontal regions, as well as the orbitofrontal clusters, are in line with previous research investigating the underlying mechanisms of approach-avoidance behavior [91, 105].

Different from the previous contrast, we also observed activity in the parahippocampal, lingual, and fusiform gyri, as well as the cuneus, which are all repeatedly reported regarding scene perception, affected by low to high-level properties [92], as well as the observer's attention [106].

To summarize, at a univariate level, the two tasks did not demonstrate significant differences in activity levels, although there are perhaps underlying differences that do not survive strict thresholds. The findings at lower thresholds indicate the categorization task engaged regions that are associated with semantic processing and affordance representations; and the approach-avoidance task engaged regions that relate to self-referential processing and egocentric point of view, reflecting the subjective nature of the task. For further examination, we conducted multivariate analyses next.

4.2 Stimulus Categories, but Not Tasks, Are Decoded at the Whole-Brain Level

Task effect was decoded at the category-selective fusiform and parahippocampal gyri at the right hemisphere, followed by small clusters at the SMAs bilaterally, then the calcarine and the medial superior frontal gyrus at the left, middle cingulate, and insula at the right hemispheres.

As we mentioned in the previous sections, these regions are essential for visual scene processing in general. Specifically, parahippocampal and fusiform gyri, also the calcarine sulcus have repeatedly been reported to be active in scene processing, and make up a portion of the scene-selective PPA and RSC, respectively [5]. These may imply that there is an effect of tasks in these scene-selective regions in the brain. The SMA, superior, medial, and inferior frontal regions, and the insula have been shown to represent information regarding the egocentric reference frames employed by the observer [95], and the significant decoding performance in these regions may reflect the different processes engaged by the tasks in our study.

However, whole-brain searchlight analyses still do not provide conclusive information regarding the task effect as these results are only observable at an uncorrected level.

On the other hand, category decoding performance was well in several brain regions, indicated by large bilateral clusters with multiple local peaks. Moreover, in a vast region with highly significant peaks at the calcarine region, the fusiform and lingual gyri, and the occipital cortex bilaterally, the decoding performance was significant for scene categories. These large clusters extended into the regions where we typically find scene-selective areas PPA, RSC, and OPA [5]. The results of this classification were in line with the previous research regarding scene categories. Fusiform and lingual gyrus, as well as parts of the calcarine gyrus and the occipital cortex, which also constitute parts of scene-selective regions, have been reported repeatedly to have good classification performances for scenes [41, 94, 107, 108]. There were also several clusters with above-chance decoding accuracy at the postcentral and precentral gyri, as well as the SMA that constitute the SMN. This may be due to our distinction of categories based on types of action. Other previously reported regions that we also observed to be good at scene category discrimination include the middle occipital cortex [41], the cuneus [107], and the cingulum [96].

These results suggest that while the task effect was not very strong at the whole-brain level, the category information regarding built environments was found in various brain areas, indicating these categories engage in several processes, modulating the activity patterns across the brain.

4.3 Activation Patterns of Scene-Selective Regions Are Affected by the Behavioral Goals of the Perceiver

Finally, to investigate the task effect at the ROI level, we conducted a model-based RSA across our three bilateral scene-selective ROIs, defined with the functional localizer session we conducted.

We found a significant correlation with the task model for the neural activation patterns in all three ROIs and none of these regions had representational similarity with either the category or the visual similarity model. These results were partly surprising since these regions were often reported to have variations in their activity patterns to scene categories, with the reliability being the highest in the PPA [11, 12].

Also, the neural RDMs were correlated closely with one another, indicating a similar modulation in these regions by task. This is also interesting; as we discussed in detail in the introduction, these scene-selective regions are reported to process various different aspects of scenes, although not exclusively. Thus, considering they share common roles and have functional connections with one another [31], these two tasks may have affected them similarly in the case of our experimental choices.

Still, despite being significantly correlated with all the neural RDMs, the task model did not reach the noise ceiling. This means that despite the evident task effect, neural activation patterns in scene-selective areas cannot be fully accounted for by task. Thus, there must be other processes that our models did not precisely represent or consider that modulate these regions. Considering the previously reported differences between PPA, RSC, and OPA that we could not support within the limits of our data and experimental procedure, perhaps there isn't a single true model to explain activity patterns in all of them.

4.4 Limitations

Dealing with high-level scene perception using ecologically valid stimuli and utilizing a categorization approach that is new to the field, this study has several limitations. In this section, I will discuss these limitations and possible solutions to address them in the future.

First of all, while we aimed to have natural, ordinary-looking stimuli by using real, unaltered photographs, these may have posed certain limitations. Firstly, we could not precisely control low-level visual properties without giving up on ecological validity. We accounted for this by including a visual model in our RSA analyses and found that the visual model was not correlated at all with any of the neural models. However, there is more to image properties than average statistics. This could be alleviated by implementing computational visual models for various brain regions that would predict actual activation patterns to stimuli; or by regressing out the image properties from the neural RDMs rather than only performing pairwise comparisons (for example: [109, 110]).

Another limitation comes from the content of the stimuli. Since we chose our stimuli from a database based on our categorization criteria, we were limited by the content of the database and could not control our stimulus content beyond their fit to our categories which may have affected the resulting activation patterns and approach-avoidance tendencies. Indeed, we observed that some stimuli elicited enter responses more, while some others elicited the opposite (Supplementary Figure A.7). Characteristics of environments previously shown to affect human brain activity and approach-avoidance decisions that we could not match across our stimuli include the geometry of the environments such as curvature, size, openness, and contours [111–113]; architectural design factors such as lighting, color, and style [114, 115]; and aesthetics [116]. Future studies may take advantage of the ever-evolving virtual reality tools to create realistic environments, which would allow controlling for various low and high-level properties while presenting the participants a variety of environments [117]. A pilot norming study to choose neutral stimuli for a balanced response ratio by obtaining behavioral ratings on specific criteria [55], or initially determining the stimuli content based on a hypothesized criteria to be able to expect a response ratio should be considered in such future studies.

Another possible limitation is related to categories. Although we employed multiple behavioral tasks which is needed more in the scene literature and applied a principled categorization approach, our tasks, and stimulus categories may have presented certain limitations. First, we only used the perspective of one categorization approach to determine our categories and also simplified it to program an experiment of ideal length. Our categories addressed the action affordances and functions of environments common to public built environments within these simplified categories. However, by doing so, we had to group environments that potentially have different semantic associations and action affordances together (entrances and exits, various circulation elements, and eating and seating areas). Future studies may improve this categorization approach and include a more comprehensive selection of environments that afford various, distinct actions by optimizing the experimental procedure.

We also identified a possible limitation due to our choice of tasks. While we aimed to examine initial responses to environments with the approach-avoidance task, and instructed participants in a way that does not emphasize positive or negative qualities that may affect these decisions, participants may still have developed their own strategies of what we may expect from them. Some participants may have decided based on their aesthetic/beauty judgments, and some may have answered based on what they would do in an environment if they were to enter. Although we were not interested in the actual answers to each environment, and thus did not perform statistical analyses on these responses, we observed variations. When we look at the enter-or-not response ratio of each participant individually, as shown in Supplementary Figure A.6, a clear difference across subjects in the tendency to enter or not can be seen. Indeed, previous research emphasizes individual variations in the approach-avoidance response ratio and possible neural activity changes due to these tendency differences [118], something we did not consider. Since we had no control over the exact strategy each subject may have recruited, our measurements could be complex in nature and therefore hard to interpret. However, previous work that compared approach-avoidance decisions to various other judgments about an environment reached the conclusion that beauty, pleasantness, comfort level, or similar judgments are not enough to explain enter-or-not decisions [112, 113]. Therefore, while we still defend that this task measured initial processing regarding *acting within* an environment, it can be improved by employing other tasks for comparison or optimizing the stimulus set by taking precautions we suggested earlier to make sure similar cognitive facilities are engaged across participants while they are performing the task.

Finally, our method of choosing the ROIs could have affected the results. We used group-level results to define common ROIs for all participants. However, functionally defined brain regions may require very liberal thresholds for some individuals to be detected, and some individuals may not have them in one or both hemispheres, whereas for some individuals, they are very large and show strong activation to relevant stimuli. This introduces additional variance and noise into the data. To address this, we tried to define relatively small clusters as ROIs at strict thresholds defining the most active region for each area across subjects. A more rigorous approach to defining thresholds at an individual level and removing those who do not fit the criteria from further analyses may have resulted in more robust findings.

4.5 Interdisciplinary Approach to Scene Perception and Future Directions

Perceiving, understanding, and acting within scenes, in our case built environments, engage multiple processes including various sensory modalities [119, 120], are influenced by endless behavioral goals [49] that depend on an individual's task, needs, physical, psychological, and neurological differences as well as countless other qualities of environments. All these phenomena are subjects of different fields individually; such as psychology, neuroscience, architecture, engineering, and possibly more. Therefore, a holistic understanding of this topic requires multidimensional examination with an interdisciplinary approach.

At first glance, scene perception and architecture seem to have a large intersection, that is, the study of built environments. Nevertheless, there seems to exist a lack of common nomenclature, a terminological disparity that is blocking the permeability between these fields, as well as significantly different paradigms or theoretical backgrounds limiting the transfer of information [121].

The scene perception literature thoroughly examines brain activity patterns to various stimulus properties, implementing scientific experimental paradigms that allow for good control of confounds. However, how we integrate various information and experience our surroundings cannot be fully understood in isolation, as people are not only passive perceivers of spaces, but they are also active agents building, interacting with, and modifying their environments [122]. On the other hand, in the architecture discipline the traditional way of solving problems and addressing human needs has been the designers' intuitions and observations, with little to no influence from the underlying brain processes and psychological responses [123, 124] despite the proven impact of architectural factors to mental and physical health [123, 125, 126].

An emerging field addressing this need, often called *neuroarchitecture*, has gained prominence recently, promoting the use of neuroscientific knowledge in the application of architectural principles to create user-friendly environments that support human cognition and well-being, in a way incorporating the body of knowledge from architecture and neuroscience into environmental psychology. Although it is not a new idea to bridge the gap between these fields [127], the related literature still lacks direction and a systematic framework; and is affected by the terminological and theoretical disparity mentioned earlier. On the one hand, scene perception research often neglects to consider architecture, which holds valuable insights into the design, construction, and influence of built environments. On the other hand, the neuroarchitecture literature attempts to bridge this gap but often falls short in terms of the experimental and analytical rigor of the former field. Despite their inseparable connection regarding the subject matter, these two fields have often operated in isolation, with limited exchange of knowledge and methodology. For example, although neuroarchitecture studies that use common stimuli [128, 129] and examine from an architectural perspective concepts that could also inform scene literature such as affective responses [130], beauty, approachability and other judgments to stimulus categories [55, 112, 113] exist, even the mention let alone ROI analyses of scene-selective regions, use of multivariate techniques, or discussion of previous findings fundamental to scene perception are hard to find, and perhaps, valuable insights into the human brain regarding architectural features that could be inferred with correct analysis methods are lost.

To overcome these limitations and reach its full potential, neuroarchitecture necessitates a paradigm shift wherein these branches converge, adopting a shared language and leveraging their respective strengths. By embracing this approach, we can unlock the full potential of neuroarchitecture, paving the way for evidence-based design principles and strategies, creating environments that are easier to navigate in, addressing individual needs, and promoting cognitive processes [131, 132]. Ultimately, combining scene perception and architecture will revolutionize our understanding of the human-environment relationship and drive the creation of built environments that positively impact individuals and communities.

4.6 Conclusion

In this study, we conducted comprehensive analyses to investigate neural activation patterns associated with built environments, an aspect often overlooked in the existing literature. Our methodology included rigorous examination of both whole-brain and ROI levels. Additionally, adopting an interdisciplinary approach, we employed a carefully selected set of stimuli based on an architectural categorization approach and incorporated multiple behavioral tasks. Our findings highlight the limitations of univariate analyses while revealing architectural category effects at the whole-brain level and task effects at the ROI level. The category classification was successful in various regions, including the lingual and parahippocampal gyri, the SMA, and the occipital cortex. The scene-selective ROIs were only significantly modulated by the task, however, the activation patterns were not explained fully by the task alone. This thesis has implications for neuroscience in terms of extending the subject matter (built environments, categories, tasks), and architectural implications in terms of studying the human-environment relationship from an interdisciplinary perspective and leveraging new research methods.

Bibliography

[1] J. M. Henderson and A. Hollingworth, “High-level scene perception,” *Annual Review of Psychology*, vol. 50, no. 1, pp. 243–271, 1999. DOI: 10.1146/annurev.psych.50.1.243.

[2] R. Epstein, A. Harris, D. Stanley, and N. Kanwisher, “The parahippocampal place area,” *Neuron*, vol. 23, no. 1, pp. 115–125, 1999. DOI: 10.1016/S0896-6273(00)80758-8.

[3] R. Epstein, “The cortical basis of visual scene processing,” *Visual Cognition*, vol. 12, no. 6, pp. 954–978, 2005. DOI: 10.1080/13506280444000607.

[4] S. Kaplan, “Environmental preference in a knowledge-seeking, knowledge-using organism.,” in *The adapted mind: Evolutionary psychology and the generation of culture.* New York, NY, US: Oxford University Press, 1992, pp. 581–598.

[5] R. A. Epstein and C. I. Baker, “Scene perception in the human brain,” 2019. DOI: 10.1146/annurev-vision-091718.

[6] S. Suzuki, F. S. Kamps, D. D. Dilks, and M. T. Treadway, “Two scene navigation systems dissociated by deliberate versus automatic processing,” *Cortex*, vol. 140, pp. 199–209, 2021. DOI: 10.1016/j.cortex.2021.03.027.

[7] R. Epstein and N. Kanwisher, “A cortical representation of the local visual environment,” *Nature*, vol. 392, no. 6676, pp. 598–601, 1998. DOI: 10.1038/33402.

[8] R. Epstein, E. A. DeYoe, D. Z. Press, A. C. Rosen, and N. Kanwisher, “Neuropsychological evidence for a topographical learning mechanism in parahippocampal cortex,” *Cognitive Neuropsychology*, vol. 18, no. 6, pp. 481–508, 2001. DOI: `10.1080/02643290125929`.

[9] S. Köhler, J. Crane, and B. Milner, “Differential contributions of the parahippocampal place area and the anterior hippocampus to human memory for scenes: MTL contributions to scene memory,” *Hippocampus*, vol. 12, no. 6, pp. 718–723, 2002. DOI: `10.1002/hipo.10077`.

[10] D. J. Kravitz, C. S. Peng, and C. I. Baker, “Real-world scene representations in high-level visual cortex: It’s the spaces more than the places,” *Journal of Neuroscience*, vol. 31, no. 20, pp. 7322–7333, 2011. DOI: `10.1523/JNEUROSCI.4588-10.2011`.

[11] A. S. Persichetti and D. D. Dilks, “Dissociable neural systems for recognizing places and navigating through them,” *The Journal of Neuroscience*, vol. 38, no. 48, pp. 10 295–10 304, 2018. DOI: `10.1523/JNEUROSCI.1200-18.2018`.

[12] A. S. Persichetti and D. D. Dilks, “Distinct representations of spatial and categorical relationships across human scene-selective cortex,” *Proceedings of the National Academy of Sciences*, vol. 116, no. 42, pp. 21 312–21 317, 2019. DOI: `10.1073/pnas.1903057116`.

[13] R. Epstein, K. S. Graham, and P. E. Downing, “Viewpoint-specific scene representations in human parahippocampal cortex,” *Neuron*, vol. 37, no. 5, pp. 865–876, 2003. DOI: `10.1016/S0896-6273(03)00117-X`.

[14] E. H. Silson, A. W.-Y. Chan, R. C. Reynolds, D. J. Kravitz, and C. I. Baker, “A retinotopic basis for the division of high-level scene processing between lateral and ventral human occipitotemporal cortex,” *Journal of Neuroscience*, vol. 35, no. 34, pp. 11 921–11 935, 2015. DOI: `10.1523/JNEUROSCI.0137-15.2015`.

[15] S. D. Auger and E. A. Maguire, “Assessing the mechanism of response in the retrosplenial cortex of good and poor navigators,” *Cortex*, vol. 49, no. 10, pp. 2904–2913, 2013. DOI: `10.1016/j.cortex.2013.08.002`.

[16] G. L. Malcolm, I. I. Groen, and C. I. Baker, "Making sense of real-world scenes," *Trends in Cognitive Sciences*, vol. 20, no. 11, pp. 843–856, 2016. DOI: `10.1016/j.tics.2016.09.003`.

[17] A. Harel, D. J. Kravitz, and C. I. Baker, "Deconstructing visual scenes in cortex: Gradients of object and spatial layout information," *Cerebral Cortex*, vol. 23, no. 4, pp. 947–957, 2013. DOI: `10.1093/cercor/bhs091`.

[18] D. D. Dilks, F. S. Kamps, and A. S. Persichetti, "Three cortical scene systems and their development," *Trends in Cognitive Sciences*, vol. 26, no. 2, pp. 117–127, 2022, Publisher: Elsevier Ltd. DOI: `10.1016/j.tics.2021.11.002`.

[19] S. D. Vann, J. P. Aggleton, and E. A. Maguire, "What does the retrosplenial cortex do?" *Nature Reviews Neuroscience*, vol. 10, no. 11, pp. 792–802, 2009. DOI: `10.1038/nrn2733`.

[20] E. Maguire, "The retrosplenial contribution to human navigation: A review of lesion and neuroimaging findings," *Scandinavian Journal of Psychology*, vol. 42, no. 3, pp. 225–238, 2001. DOI: `10.1111/1467-9450.00233`.

[21] M. E. Raichle, "The brain's default mode network," *Annual Review of Neuroscience*, vol. 38, no. 1, pp. 433–447, 2015. DOI: `10.1146/annurev-neuro-071013-014030`.

[22] D. D. Dilks, J. B. Julian, J. Kubilius, E. S. Spelke, and N. Kanwisher, "Mirror-image sensitivity and invariance in object and scene processing pathways," *Journal of Neuroscience*, vol. 31, no. 31, pp. 11 305–11 312, 2011. DOI: `10.1523/JNEUROSCI.1935-11.2011`.

[23] S. D. Auger, S. L. Mullally, and E. A. Maguire, "Retrosplenial cortex codes for permanent landmarks," *PLoS ONE*, vol. 7, no. 8, C. I. Baker, Ed., e43620, 2012. DOI: `10.1371/journal.pone.0043620`.

[24] S. A. Marchette, L. K. Vass, J. Ryan, and R. A. Epstein, "Anchoring the neural compass: Coding of local spatial reference frames in human medial parietal lobe," *Nature Neuroscience*, vol. 17, no. 11, pp. 1598–1606, 2014, Publisher: Nature Publishing Group. DOI: `10.1038/nn.3834`.

[25] S. A. Marchette, L. K. Vass, J. Ryan, and R. A. Epstein, "Outside looking in: Landmark generalization in the human navigational system," *Journal of Neuroscience*, vol. 35, no. 44, pp. 14 896–14 908, 2015. DOI: `10.1523/JNEUROSCI.2270-15.2015`.

[26] R. A. Epstein, W. E. Parker, and A. M. Feiler, "Where am i now? distinct roles for parahippocampal and retrosplenial cortices in place recognition," *Journal of Neuroscience*, vol. 27, no. 23, pp. 6141–6149, 2007. DOI: `10.1523/JNEUROSCI.0799-07.2007`.

[27] R. A. Epstein, J. S. Higgins, K. Jablonski, and A. M. Feiler, "Visual scene processing in familiar and unfamiliar environments," *Journal of Neurophysiology*, vol. 97, no. 5, pp. 3670–3683, 2007. DOI: `10.1152/jn.00003.2007`.

[28] A. S. Alexander, R. Place, M. J. Starrett, E. R. Chrastil, and D. A. Nitz, "Rethinking retrosplenial cortex: Perspectives and predictions," *Neuron*, S0896627322010273, 2022. DOI: `10.1016/j.neuron.2022.11.006`.

[29] V. Troiani, A. Stigliani, M. E. Smith, and R. A. Epstein, "Multiple object properties drive scene-selective regions," *Cerebral Cortex*, vol. 24, no. 4, pp. 883–897, 2014. DOI: `10.1093/cercor/bhs364`.

[30] M. Stacho and D. Manahan-Vaughan, "Mechanistic flexibility of the retrosplenial cortex enables its contribution to spatial cognition," *Trends in Neurosciences*, vol. 45, no. 4, pp. 284–296, 2022. DOI: `10.1016/j.tins.2022.01.007`.

[31] D. D. Dilks, J. B. Julian, A. M. Paunov, and N. Kanwisher, "The occipital place area is causally and selectively involved in scene perception," *The Journal of Neuroscience*, vol. 33, no. 4, pp. 1331–1336, 2013. DOI: `10.1523/JNEUROSCI.4081-12.2013`.

[32] A. Steel, M. M. Billings, E. H. Silson, and C. E. Robertson, "A network linking scene perception and spatial memory systems in posterior cerebral cortex," *Nature Communications*, vol. 12, no. 1, p. 2632, 2021. DOI: `10.1038/s41467-021-22848-z`.

[33] F. S. Kamps, J. B. Julian, J. Kubilius, N. Kanwisher, and D. D. Dilks, "The occipital place area represents the local elements of scenes," *NeuroImage*, vol. 132, pp. 417–424, 2016. DOI: `10.1016/j.neuroimage.2016.02.062`.

[34] L. Henriksson, M. Mur, and N. Kriegeskorte, "Rapid invariant encoding of scene layout in human OPA," *Neuron*, vol. 103, no. 1, 161–171.e3, 2019. DOI: `10.1016/j.neuron.2019.04.014`.

[35] J. B. Julian, J. Ryan, R. H. Hamilton, and R. A. Epstein, "The occipital place area is causally involved in representing environmental boundaries during navigation," *Current Biology*, vol. 26, no. 8, pp. 1104–1109, 2016. DOI: `10.1016/j.cub.2016.02.066`.

[36] J. M. Henderson, C. L. Larson, and D. C. Zhu, "Cortical activation to indoor versus outdoor scenes: An fMRI study," *Experimental Brain Research*, vol. 179, no. 1, pp. 75–84, 2007. DOI: `10.1007/s00221-006-0766-2`.

[37] G. Rousselet, O. Joubert, and M. Fabre-Thorpe, "How long to get to the "gist" of real-world natural scenes?" *Visual Cognition*, vol. 12, no. 6, pp. 852–877, 2005. DOI: `10.1080/13506280444000553`.

[38] M. N. Gopnarayan, D. R. Rathore, F. S. Bauer, J. Hillard, and P. Chawla, "Differential representation of natural and manmade images in the human ventral visual stream," Neuroscience, preprint, 2022. DOI: `10.1101/2022.09.22.509086`.

[39] I. I. A. Groen, S. Ghebreab, H. Prins, V. A. F. Lamme, and H. S. Scholte, "From image statistics to scene gist: Evoked neural activity reveals transition from low-level natural image structure to scene category," *Journal of Neuroscience*, vol. 33, no. 48, pp. 18 814–18 824, 2013. DOI: `10.1523/JNEUROSCI.3128-13.2013`.

[40] M. R. Greene and B. C. Hansen, "Disentangling the independent contributions of visual and conceptual features to the spatiotemporal dynamics of scene categorization," *Journal of Neuroscience*, vol. 40, no. 27, pp. 5283–5299, 2020, Publisher: Society for Neuroscience. DOI: `10.1523/JNEUROSCI.2088-19.2020`.

[41] M. R. Johnson and M. K. Johnson, "Decoding individual natural scene representations during perception and imagery," *Frontiers in Human Neuroscience*, vol. 8, 2014. DOI: `10.3389/fnhum.2014.00059`.

[42] M. Greene and A. Oliva, "Recognition of natural scenes from global properties: Seeing the forest without representing the trees," *Cognitive Psychology*, vol. 58, no. 2, pp. 137–176, 2009. DOI: `10.1016/j.cogpsych.2008.06.001`.

[43] A. Oliva and A. Torralba, "Modeling the shape of the scene: A holistic representation of the spatial envelope," *International Journal of Computer Vision*, vol. 42, pp. 145–175, 2001.

[44] M. McCotter, F. Gosselin, P. Sowden, and P. Schyns, "The use of visual information in natural scenes," *Visual Cognition*, vol. 12, no. 6, pp. 938–953, 2005. DOI: `10.1080/13506280444000599`.

[45] D. Kaping, T. Tzvetanov, and S. Treue, "Adaptation to statistical properties of visual scenes biases rapid categorization," *Visual Cognition*, vol. 15, no. 1, pp. 12–19, 2007. DOI: `10.1080/13506280600856660`.

[46] A. Oliva and P. G. Schyns, "Diagnostic colors mediate scene recognition," *Cognitive Psychology*, vol. 41, no. 2, pp. 176–210, 2000. DOI: `10.1006/cogp.1999.0728`.

[47] M. R. Greene and A. Oliva, "The briefest of glances: The time course of natural scene understanding," *Psychological Science*, vol. 20, no. 4, pp. 464–472, 2009. DOI: `10.1111/j.1467-9280.2009.02316.x`.

[48] M. F. Bonner and R. A. Epstein, "Coding of navigational affordances in the human visual system," *Proceedings of the National Academy of Sciences of the United States of America*, vol. 114, no. 18, pp. 4793–4798, 2017, Publisher: National Academy of Sciences. DOI: `10.1073/pnas.1618228114`.

[49] I. I. Groen, E. H. Silson, and C. I. Baker, "Contributions of low- and high-level properties to neural processing of visual scenes in the human brain," *Philosophical Transactions of the Royal Society B: Biological Sciences*, vol. 372, no. 1714, 2017, Publisher: Royal Society. DOI: `10.1098/rstb.2016.0102`.

[50] N. E. Klepeis *et al.*, "The national human activity pattern survey (NHAPS): A resource for assessing exposure to environmental pollutants," *Journal of Exposure Science & Environmental Epidemiology*, vol. 11, no. 3, pp. 231–252, 2001. DOI: `10.1038/sj.jea.7500165`.

[51] N. L. Cholowsky *et al.*, "Consequences of changing canadian activity patterns since the COVID-19 pandemic include increased residential radon gas exposure for younger people," *Scientific Reports*, vol. 13, no. 1, p. 5735, 2023. DOI: `10.1038/s41598-023-32416-8`.

[52] P. B. Bryan, J. B. Julian, and R. A. Epstein, "Rectilinear edge selectivity is insufficient to explain the category selectivity of the parahippocampal place area," *Frontiers in Human Neuroscience*, vol. 10, 2016. DOI: `10.3389/fnhum.2016.00137`.

[53] I. I. Groen, M. R. Greene, C. Baldassano, L. Fei-Fei, D. M. Beck, and C. I. Baker, "Distinct contributions of functional and deep neural network features to representational similarity of scenes in human brain and behavior," *eLife*, vol. 7, 2018. DOI: `10.7554/eLife.32962`.

[54] Y. Jung and D. B. Walther, "Neural representations in the prefrontal cortex are task dependent for scene attributes but not for scene categories," *The Journal of Neuroscience*, vol. 41, no. 34, pp. 7234–7245, 2021. DOI: `10.1523/JNEUROSCI.2816-20.2021`.

[55] A. Coburn *et al.*, "Psychological and neural responses to architectural interiors," *Cortex*, vol. 126, pp. 217–241, 2020. DOI: `10.1016/j.cortex.2020.01.009`.

[56] H. Froyen, *Universal Design, a methodological approach: A pathway to human-friendly and elegant architecture*. Institute for Human Centered Design, 2012.

[57] J. Xiao, J. Hays, K. A. Ehinger, A. Oliva, and A. Torralba, "SUN database: Large-scale scene recognition from abbey to zoo," in *2010 IEEE Computer Society Conference on Computer Vision and Pattern Recognition*, IEEE, 2010, pp. 3485–3492. DOI: `10.1109/CVPR.2010.5539970`.

[58] J. Xiao, K. A. Ehinger, J. Hays, A. Torralba, and A. Oliva, “SUN database: Exploring a large collection of scene categories,” *International Journal of Computer Vision*, vol. 119, no. 1, pp. 3–22, 2016. DOI: `10.1007/s11263-014-0748-y`.

[59] R. M. Korn and A. J. Elliot, “Avoidance and approach motivation: A brief history,” in *International Encyclopedia of the Social & Behavioral Sciences*, Elsevier, 2015, pp. 326–331. DOI: `10.1016/B978-0-08-097086-8.26071-6`.

[60] D. H. Brainard, “The psychophysics toolbox.,” *Spatial vision*, vol. 10, no. 4, pp. 433–436, 1997, Place: Netherlands.

[61] D. G. Pelli, “The videotoolbox software for visual psychophysics: Transforming numbers into movies,” *Spatial Vision*, vol. 10, no. 4, pp. 437–442, 1997. DOI: `https://doi.org/10.1163/156856897X00366`.

[62] M. Kleiner, D. H. Brainard, and D. Pelli, “What’s new in psychtoolbox-3?” *Perception*, vol. 36, pp. 1–16, 2007.

[63] T. W. Meissner, M. Nordt, and S. Weigelt, “Prolonged functional development of the parahippocampal place area and occipital place area,” *NeuroImage*, vol. 191, pp. 104–115, 2019. DOI: `10.1016/j.neuroimage.2019.02.025`.

[64] O. Esteban *et al.*, “Fmriprep,” *Software*, 2018. DOI: `10.5281/zenodo.852659`.

[65] O. Esteban *et al.*, “fMRIPrep: A robust preprocessing pipeline for functional MRI,” *Nature Methods*, 2018. DOI: `10.1038/s41592-018-0235-4`.

[66] K. Gorgolewski *et al.*, “Nipype: A flexible, lightweight and extensible neuroimaging data processing framework in python,” *Frontiers in Neuroinformatics*, vol. 5, p. 13, 2011. DOI: `10.3389/fninf.2011.00013`.

[67] K. J. Gorgolewski *et al.*, “Nipype,” *Software*, 2018. DOI: `10.5281/zenodo.596855`.

[68] N. J. Tustison *et al.*, “N4itk: Improved n3 bias correction,” *IEEE Transactions on Medical Imaging*, vol. 29, no. 6, pp. 1310–1320, 2010. DOI: `10.1109/TMI.2010.2046908`.

[69] B. Avants, C. Epstein, M. Grossman, and J. Gee, "Symmetric diffeomorphic image registration with cross-correlation: Evaluating automated labeling of elderly and neurodegenerative brain," *Medical Image Analysis*, vol. 12, no. 1, pp. 26–41, 2008. DOI: `10.1016/j.media.2007.06.004`.

[70] Y. Zhang, M. Brady, and S. Smith, "Segmentation of brain MR images through a hidden markov random field model and the expectation-maximization algorithm," *IEEE Transactions on Medical Imaging*, vol. 20, no. 1, pp. 45–57, 2001. DOI: `10.1109/42.906424`.

[71] M. Reuter, H. D. Rosas, and B. Fischl, "Highly accurate inverse consistent registration: A robust approach," *NeuroImage*, vol. 53, no. 4, pp. 1181–1196, 2010. DOI: `10.1016/j.neuroimage.2010.07.020`.

[72] A. M. Dale, B. Fischl, and M. I. Sereno, "Cortical surface-based analysis: I. segmentation and surface reconstruction," *NeuroImage*, vol. 9, no. 2, pp. 179–194, 1999. DOI: `10.1006/nimg.1998.0395`.

[73] A. Klein *et al.*, "Mindboggling morphometry of human brains," *PLOS Computational Biology*, vol. 13, no. 2, e1005350, 2017. DOI: `10.1371/journal.pcbi.1005350`.

[74] V. Fonov, A. Evans, R. McKinstry, C. Almli, and D. Collins, "Unbiased nonlinear average age-appropriate brain templates from birth to adulthood," *NeuroImage*, vol. 47, Supplement 1, S102, 2009. DOI: `10.1016/S1053-8119(09)70884-5`.

[75] M. Jenkinson, P. Bannister, M. Brady, and S. Smith, "Improved optimization for the robust and accurate linear registration and motion correction of brain images," *NeuroImage*, vol. 17, no. 2, pp. 825–841, 2002. DOI: `10.1006/nimg.2002.1132`.

[76] R. W. Cox and J. S. Hyde, "Software tools for analysis and visualization of fmri data," *NMR in Biomedicine*, vol. 10, no. 4-5, pp. 171–178, 1997. DOI: `10.1002/(SICI)1099-1492(199706/08)10:4/5<171::AID-NBM453>3.0.CO;2-L`.

[77] D. N. Greve and B. Fischl, "Accurate and robust brain image alignment using boundary-based registration," *NeuroImage*, vol. 48, no. 1, pp. 63–72, 2009. DOI: `10.1016/j.neuroimage.2009.06.060`.

[78] J. D. Power, A. Mitra, T. O. Laumann, A. Z. Snyder, B. L. Schlaggar, and S. E. Petersen, "Methods to detect, characterize, and remove motion artifact in resting state fmri," *NeuroImage*, vol. 84, no. Supplement C, pp. 320–341, 2014. DOI: `10.1016/j.neuroimage.2013.08.048`.

[79] Y. Behzadi, K. Restom, J. Liau, and T. T. Liu, "A component based noise correction method (CompCor) for BOLD and perfusion based fmri," *NeuroImage*, vol. 37, no. 1, pp. 90–101, 2007. DOI: `10.1016/j.neuroimage.2007.04.042`.

[80] T. D. Satterthwaite *et al.*, "An improved framework for confound regression and filtering for control of motion artifact in the preprocessing of resting-state functional connectivity data," *NeuroImage*, vol. 64, no. 1, pp. 240–256, 2013. DOI: `10.1016/j.neuroimage.2012.08.052`.

[81] C. Lanczos, "Evaluation of noisy data," *Journal of the Society for Industrial and Applied Mathematics Series B Numerical Analysis*, vol. 1, no. 1, pp. 76–85, 1964. DOI: `10.1137/0701007`.

[82] M. N. Hebart, K. Görgen, and J.-D. Haynes, "The decoding toolbox (TDT): A versatile software package for multivariate analyses of functional imaging data," *Frontiers in Neuroinformatics*, vol. 8, 2015. DOI: `10.3389/fninf.2014.00088`.

[83] C.-C. Chang and C.-J. Lin, "LIBSVM: A library for support vector machines," *ACM Transactions on Intelligent Systems and Technology*, vol. 2, no. 3, pp. 1–27, 2011. DOI: `10.1145/1961189.1961199`.

[84] N. Kriegeskorte, R. Goebel, and P. Bandettini, "Information-based functional brain mapping," *Proceedings of the National Academy of Sciences*, vol. 103, no. 10, pp. 3863–3868, 2006. DOI: `10.1073/pnas.0600244103`.

[85] J. Julian, E. Fedorenko, J. Webster, and N. Kanwisher, "An algorithmic method for functionally defining regions of interest in the ventral visual

pathway," *NeuroImage*, vol. 60, no. 4, pp. 2357–2364, 2012. DOI: `10.1016/j.neuroimage.2012.02.055`.

[86] M. Brett, J.-L. Anton, R. Valabrègue, and J. B. Poline, "Region of interest analysis using an SPM toolbox," 2010.

[87] N. Kriegeskorte, "Representational similarity analysis – connecting the branches of systems neuroscience," *Frontiers in Systems Neuroscience*, 2008. DOI: `10.3389/neuro.06.004.2008`.

[88] H. Nili, C. Wingfield, A. Walther, L. Su, W. Marslen-Wilson, and N. Kriegeskorte, "A toolbox for representational similarity analysis," *PLoS Computational Biology*, vol. 10, no. 4, 2014, Publisher: Public Library of Science. DOI: `10.1371/journal.pcbi.1003553`.

[89] D. S. Marcus *et al.*, "Human connectome project informatics: Quality control, database services, and data visualization," *NeuroImage*, vol. 80, pp. 202–219, 2013, Mapping the Connectome. DOI: `https://doi.org/10.1016/j.neuroimage.2013.05.077`.

[90] R. J. Binney, K. V. Embleton, E. Jefferies, G. J. M. Parker, and M. A. Lambon Ralph, "The ventral and inferolateral aspects of the anterior temporal lobe are crucial in semantic memory: Evidence from a novel direct comparison of distortion-corrected fMRI, rTMS, and semantic dementia," *Cerebral Cortex*, vol. 20, no. 11, pp. 2728–2738, 2010. DOI: `10.1093/cercor/bhq019`.

[91] J. M. Spielberg *et al.*, "A brain network instantiating approach and avoidance motivation: Network instantiating motivation," *Psychophysiology*, vol. 49, no. 9, pp. 1200–1214, 2012. DOI: `10.1111/j.1469-8986.2012.01443.x`.

[92] L. Kauffmann, S. RamanoÃ«l, and C. Peyrin, "The neural bases of spatial frequency processing during scene perception," *Frontiers in Integrative Neuroscience*, vol. 8, 2014. DOI: `10.3389/fnint.2014.00037`.

[93] D. B. Walther, E. Caddigan, L. Fei-Fei, and D. M. Beck, "Natural scene categories revealed in distributed patterns of activity in the human brain,"

Journal of Neuroscience, vol. 29, no. 34, pp. 10 573–10 581, 2009. DOI: `10.1523/JNEUROSCI.0559-09.2009`.

[94] H. M. Bonnici, D. Kumaran, M. J. Chadwick, N. Weiskopf, D. Hassabis, and E. A. Maguire, “Decoding representations of scenes in the medial temporal lobes,” *Hippocampus*, vol. 22, no. 5, pp. 1143–1153, 2012. DOI: `10.1002/hipo.20960`.

[95] A. Saj, Y. Cojan, B. Musel, J. Honoré, L. Borel, and P. Vuilleumier, “Functional neuro-anatomy of egocentric versus allocentric space representation,” *Neurophysiologie Clinique/Clinical Neurophysiology*, vol. 44, no. 1, pp. 33–40, 2014. DOI: `10.1016/j.neucli.2013.10.135`.

[96] Y. Jung, B. Larsen, and D. B. Walther, “Modality-independent coding of scene categories in prefrontal cortex,” *The Journal of Neuroscience*, vol. 38, no. 26, pp. 5969–5981, 2018. DOI: `10.1523/JNEUROSCI.0272-18.2018`.

[97] X. Wang *et al.*, “Decoding natural scenes based on sounds of objects within scenes using multivariate pattern analysis,” *Neuroscience Research*, vol. 148, pp. 9–18, 2019. DOI: `10.1016/j.neures.2018.11.009`.

[98] G. Galati, G. Pelle, A. Berthoz, and G. Committeri, “Multiple reference frames used by the human brain for spatial perception and memory,” *Experimental Brain Research*, vol. 206, no. 2, pp. 109–120, 2010. DOI: `10.1007/s00221-010-2168-8`.

[99] M. Van Assche, V. Kebets, P. Vuilleumier, and F. Assal, “Functional dissociations within posterior parietal cortex during scene integration and viewpoint changes,” *Cerebral Cortex*, bhu215, 2014. DOI: `10.1093/cercor/bhu215`.

[100] P. Zeidman, S. L. Mullally, and E. A. Maguire, “Constructing, perceiving, and maintaining scenes: Hippocampal activity and connectivity,” *Cerebral Cortex*, vol. 25, no. 10, pp. 3836–3855, 2015. DOI: `10.1093/cercor/bhu266`.

[101] S. Thill, D. Caligiore, A. M. Borghi, T. Ziemke, and G. Baldassarre, "Theories and computational models of affordance and mirror systems: An integrative review," *Neuroscience & Biobehavioral Reviews*, vol. 37, no. 3, pp. 491–521, 2013. DOI: `10.1016/j.neubiorev.2013.01.012`.

[102] D. J. Kravitz, K. S. Saleem, C. I. Baker, and M. Mishkin, "A new neural framework for visuospatial processing," *Nature Reviews Neuroscience*, vol. 12, no. 4, pp. 217–230, 2011. DOI: `10.1038/nrn3008`.

[103] L. Q. Uddin, B. T. T. Yeo, and R. N. Spreng, "Towards a universal taxonomy of macro-scale functional human brain networks," *Brain Topography*, vol. 32, no. 6, pp. 926–942, 2019. DOI: `10.1007/s10548-019-00744-6`.

[104] J. S. Cant and M. A. Goodale, "Attention to form or surface properties modulates different regions of human occipitotemporal cortex," *Cerebral Cortex*, vol. 17, no. 3, pp. 713–731, 2007. DOI: `10.1093/cercor/bhk022`.

[105] R. L. Aupperle, A. J. Melrose, A. Francisco, M. P. Paulus, and M. B. Stein, "Neural substrates of approach-avoidance conflict decision-making: Approach-avoidance conflict," *Human Brain Mapping*, vol. 36, no. 2, pp. 449–462, 2015. DOI: `10.1002/hbm.22639`.

[106] J. M. Henderson and W. Choi, "Neural correlates of fixation duration during real-world scene viewing: Evidence from fixation-related (FIRE) fMRI," *Journal of Cognitive Neuroscience*, vol. 27, no. 6, pp. 1137–1145, 2015. DOI: `10.1162/jocn_a_00769`.

[107] P. Ramkumar, B. C. Hansen, S. Pannasch, and L. C. Loschky, "Visual information representation and rapid-scene categorization are simultaneous across cortex: An MEG study," *NeuroImage*, vol. 134, pp. 295–304, 2016. DOI: `10.1016/j.neuroimage.2016.03.027`.

[108] S.-H. Lee, D. J. Kravitz, and C. I. Baker, "Disentangling visual imagery and perception of real-world objects," *NeuroImage*, vol. 59, no. 4, pp. 4064–4073, 2012. DOI: `10.1016/j.neuroimage.2011.10.055`.

[109] R. Tucciarelli, M. Wurm, E. Baccolo, and A. Lingnau, "The representational space of observed actions," *eLife*, vol. 8, e47686, 2019. DOI: `10.7554/eLife.47686`.

[110] K. Dwivedi, R. M. Cichy, and G. Roig, “Unraveling representations in scene-selective brain regions using scene-parsing deep neural networks,” *Journal of Cognitive Neuroscience*, vol. 33, no. 10, pp. 2032–2043, 2021. DOI: `10.1162/jocn_a_01624`.

[111] A. Shemesh, G. Leisman, M. Bar, and Y. J. Grobman, “A neurocognitive study of the emotional impact of geometrical criteria of architectural space,” *Architectural Science Review*, vol. 64, no. 4, pp. 394–407, 2021. DOI: `10.1080/00038628.2021.1940827`.

[112] O. Vartanian *et al.*, “Impact of contour on aesthetic judgments and approach-avoidance decisions in architecture,” *Proceedings of the National Academy of Sciences*, vol. 110, pp. 10 446–10 453, supplement_2 2013. DOI: `10.1073/pnas.1301227110`.

[113] O. Vartanian *et al.*, “Architectural design and the brain: Effects of ceiling height and perceived enclosure on beauty judgments and approach-avoidance decisions,” *Journal of Environmental Psychology*, vol. 41, pp. 10–18, 2015. DOI: `10.1016/j.jenvp.2014.11.006`.

[114] I. Bower, R. Tucker, and P. G. Enticott, “Impact of built environment design on emotion measured via neurophysiological correlates and subjective indicators: A systematic review,” *Journal of Environmental Psychology*, vol. 66, p. 101 344, 2019. DOI: `10.1016/j.jenvp.2019.101344`.

[115] H. Choo, J. L. Nasar, B. Nikrahei, and D. B. Walther, “Neural codes of seeing architectural styles,” *Scientific Reports*, vol. 7, no. 1, p. 40 201, 2017. DOI: `10.1038/srep40201`.

[116] B. Zheng and L. Gao, “Aesthetic difference of artistic design: An analysis based on brain neuroscience,” *REVISTA ARGENTINA DE CLINICA PSICOLOGICA*, 2020. DOI: `10.24205/03276716.2020.355`.

[117] M. Portman, A. Natapov, and D. Fisher-Gewirtzman, “To go where no man has gone before: Virtual reality in architecture, landscape architecture and environmental planning,” *Computers, Environment and Urban Systems*, vol. 54, pp. 376–384, 2015. DOI: `10.1016/j.compenvurbsys.2015.05.001`.

[118] J. M. Spielberg *et al.*, "Trait approach and avoidance motivation: Lateralized neural activity associated with executive function," *NeuroImage*, vol. 54, no. 1, pp. 661–670, 2011. DOI: `10.1016/j.neuroimage.2010.08.037`.

[119] A. Coburn, O. Vartanian, and A. Chatterjee, "Buildings, beauty, and the brain: A neuroscience of architectural experience," *Journal of Cognitive Neuroscience*, vol. 29, no. 9, pp. 1521–1531, 2017. DOI: `10.1162/jocn_a_01146`.

[120] C. Spence, "Senses of place: Architectural design for the multisensory mind," *Cognitive Research: Principles and Implications*, vol. 5, no. 1, p. 46, 2020. DOI: `10.1186/s41235-020-00243-4`.

[121] J. P. Eberhard, *Brain Landscape: The Coexistence of Neuroscience and Architecture*. Oxford University Press, 2009. DOI: `10.1093/acprof:oso/9780195331721.001.0001`.

[122] R. Gifford, "Environmental psychology matters," *Annual Review of Psychology*, vol. 65, no. 1, pp. 541–579, 2014. DOI: `10.1146/annurev-psych-010213-115048`.

[123] S. Azzazy, A. Ghaffarianhoseini, A. GhaffarianHoseini, N. Naismith, and Z. Doborjeh, "A critical review on the impact of built environment on users' measured brain activity," *Architectural Science Review*, vol. 64, no. 4, pp. 319–335, 2021. DOI: `10.1080/00038628.2020.1749980`.

[124] J. L. Higuera-Trujillo, C. Llinares, and E. Macagno, "The cognitive-emotional design and study of architectural space: A scoping review of neuroarchitecture and its precursor approaches," *Sensors*, vol. 21, no. 6, p. 2193, 2021. DOI: `10.3390/s21062193`.

[125] C. J. Beemer *et al.*, "A brief review on the mental health for select elements of the built environment," *Indoor and Built Environment*, vol. 30, no. 2, pp. 152–165, 2021. DOI: `10.1177/1420326X19889653`.

[126] M. F. Norwood, A. Lakhani, A. Maujean, H. Zeeman, O. Creux, and E. Kendall, "Brain activity, underlying mood and the environment: A systematic review," *Journal of Environmental Psychology*, vol. 65, pp. 101 321–101 321, 2019. DOI: `10.1016/j.jenvp.2019.101321`.

[127] J. P. Eberhard, "Applying neuroscience to architecture," *Neuron*, vol. 62, no. 6, pp. 753–756, 2009. DOI: `10.1016/j.neuron.2009.06.001`.

[128] I.-C. Tang *et al.*, "Using functional magnetic resonance imaging (fMRI) to analyze brain region activity when viewing landscapes," *Landscape and Urban Planning*, vol. 162, pp. 137–144, 2017. DOI: `10.1016/j.landurbplan.2017.02.007`.

[129] T.-H. Kim *et al.*, "Human brain activation in response to visual stimulation with rural and urban scenery pictures: A functional magnetic resonance imaging study," *Science of The Total Environment*, vol. 408, no. 12, pp. 2600–2607, 2010. DOI: `10.1016/j.scitotenv.2010.02.025`.

[130] J. Martínez-Soto, L. Gonzales-Santos, E. Pasaye, and F. A. Barrios, "Exploration of neural correlates of restorative environment exposure through functional magnetic resonance," *Intelligent Buildings International*, vol. 5, pp. 10–28, sup1 2013. DOI: `10.1080/17508975.2013.807765`.

[131] K. Jeffery, "Urban architecture: A cognitive neuroscience perspective," *The Design Journal*, vol. 22, no. 6, pp. 853–872, 2019. DOI: `10.1080/14606925.2019.1662666`.

[132] K. Jeffery, W. Guo, D. Ball, and J. Rodriguez-Sanchez, "Visual imagination and cognitive mapping of a virtual building," *Journal of Navigation*, vol. 75, no. 1, pp. 1–14, 2022. DOI: `10.1017/S0373463321000588`.

Appendix A

Supplementary Data

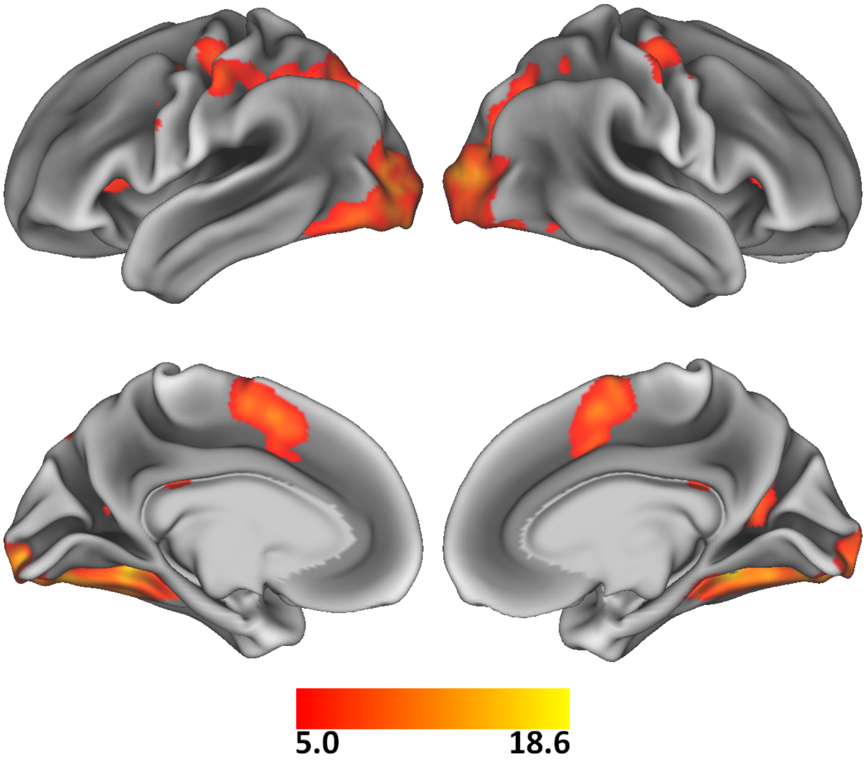

Figure A.1: **Activation map for all tasks > rest.** The results were at $p<0.05$ (FWE-corrected).

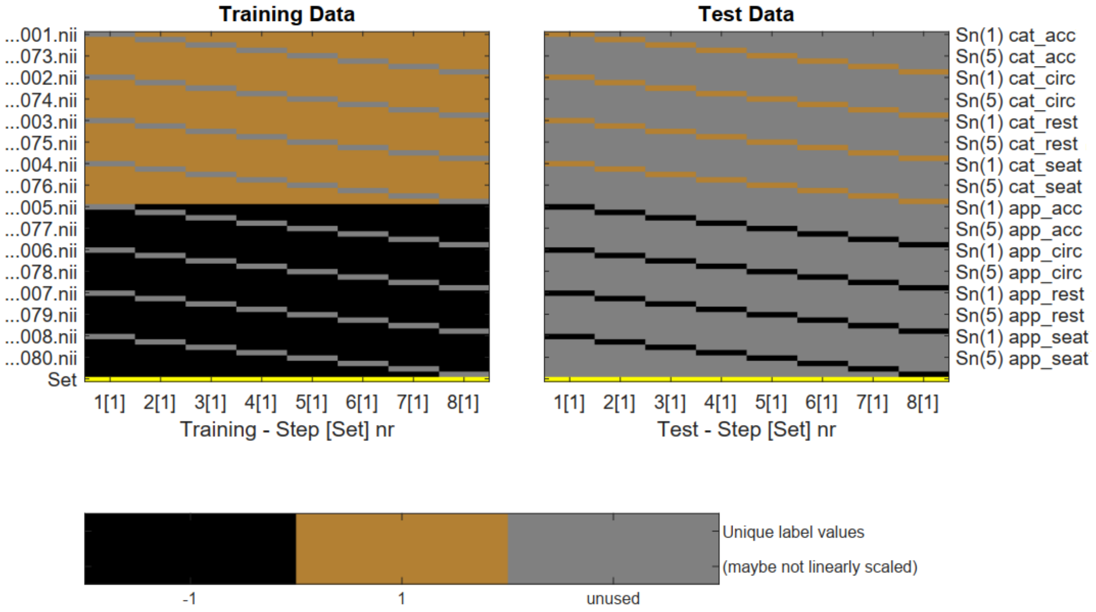

Figure A.2: **MVPA design: task classification.**

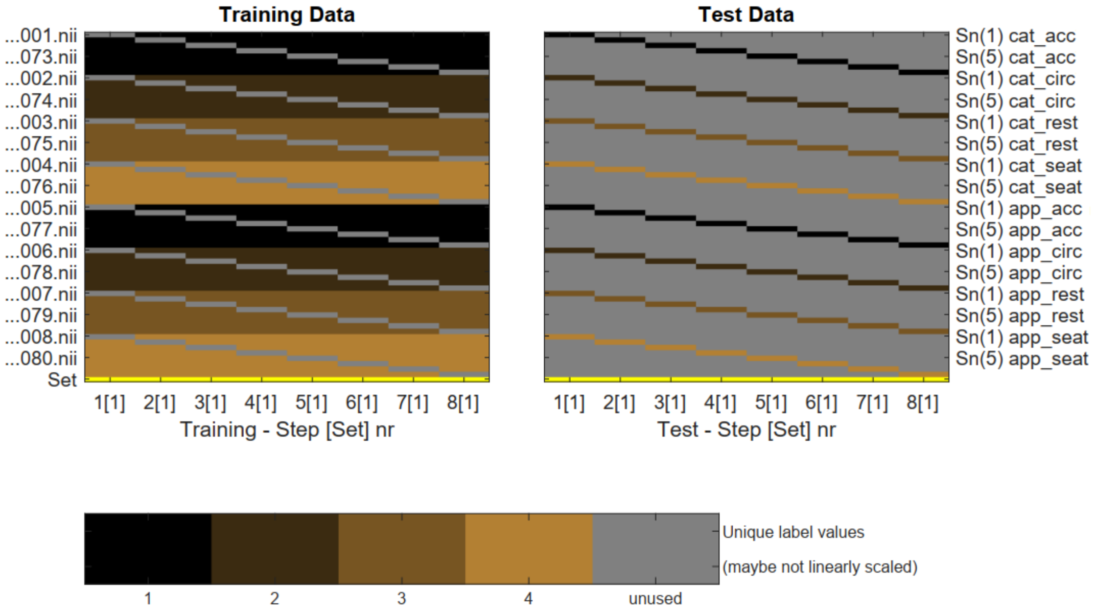

Figure A.3: **MVPA design: category classification.**

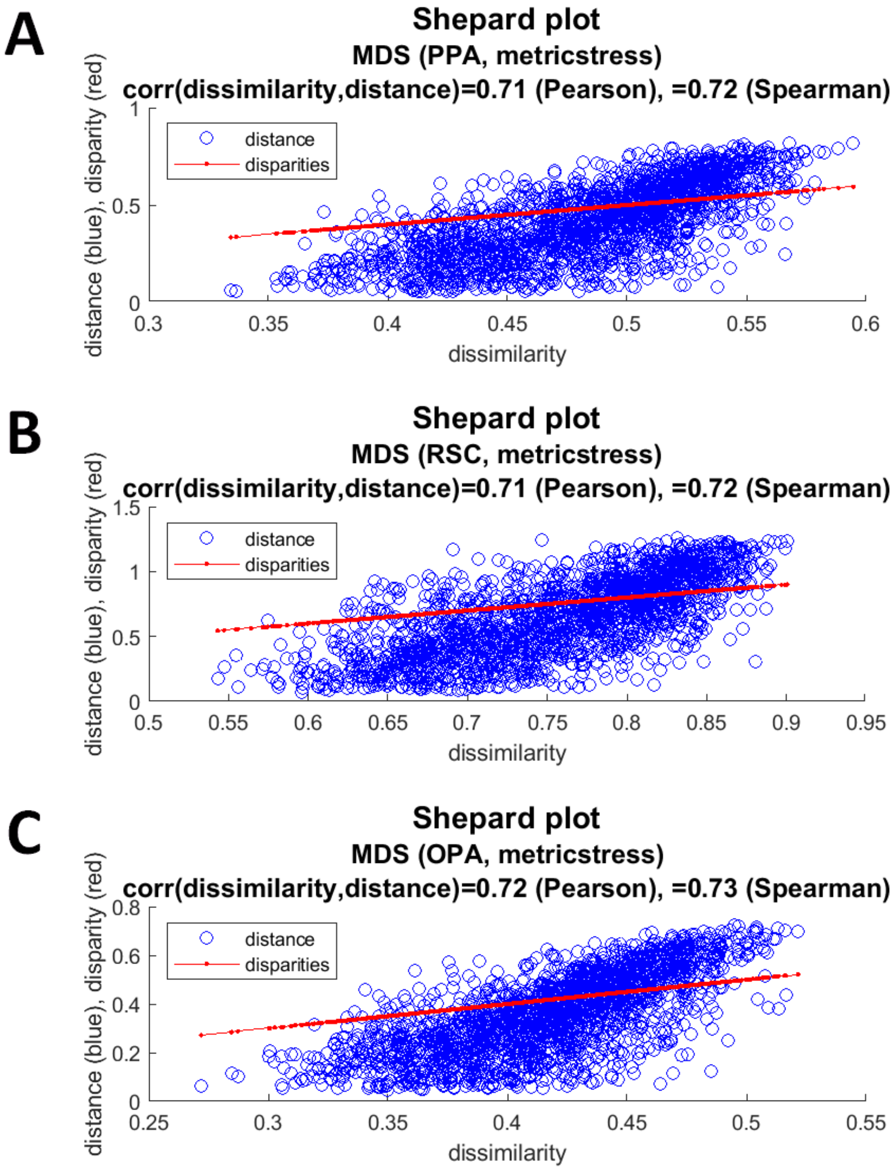

Figure A.4: **MDS Shepard plots, A-PPA, B-RSC, C-OPA.** Scatter plots showing the dissimilarities and disparities.

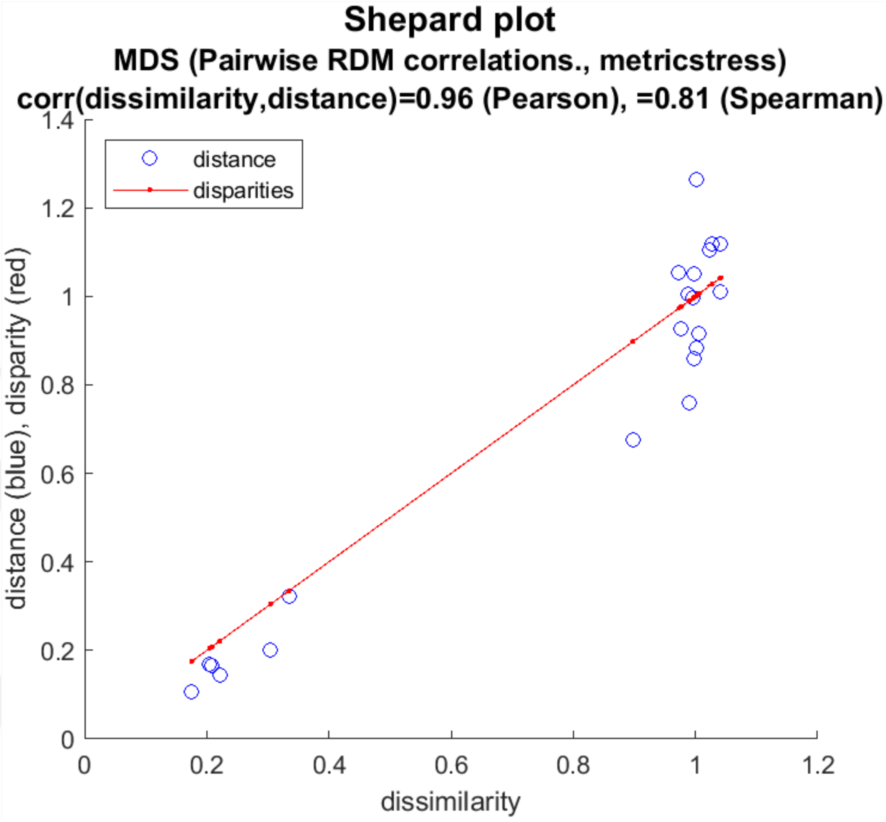

Figure A.5: **Pairwise RDM correlations MDS Shepard plot.** Scatter plot showing the dissimilarities and disparities.

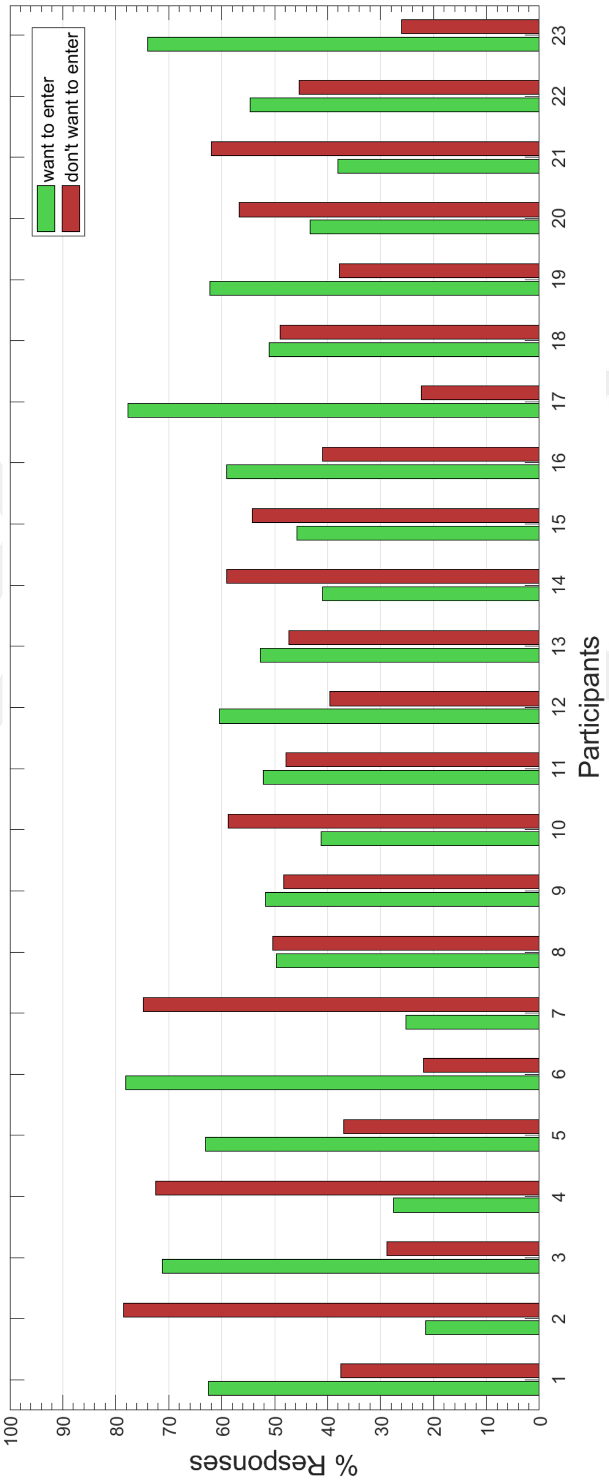

Figure A.6: **Ratio of approach/avoidance responses by subject.**

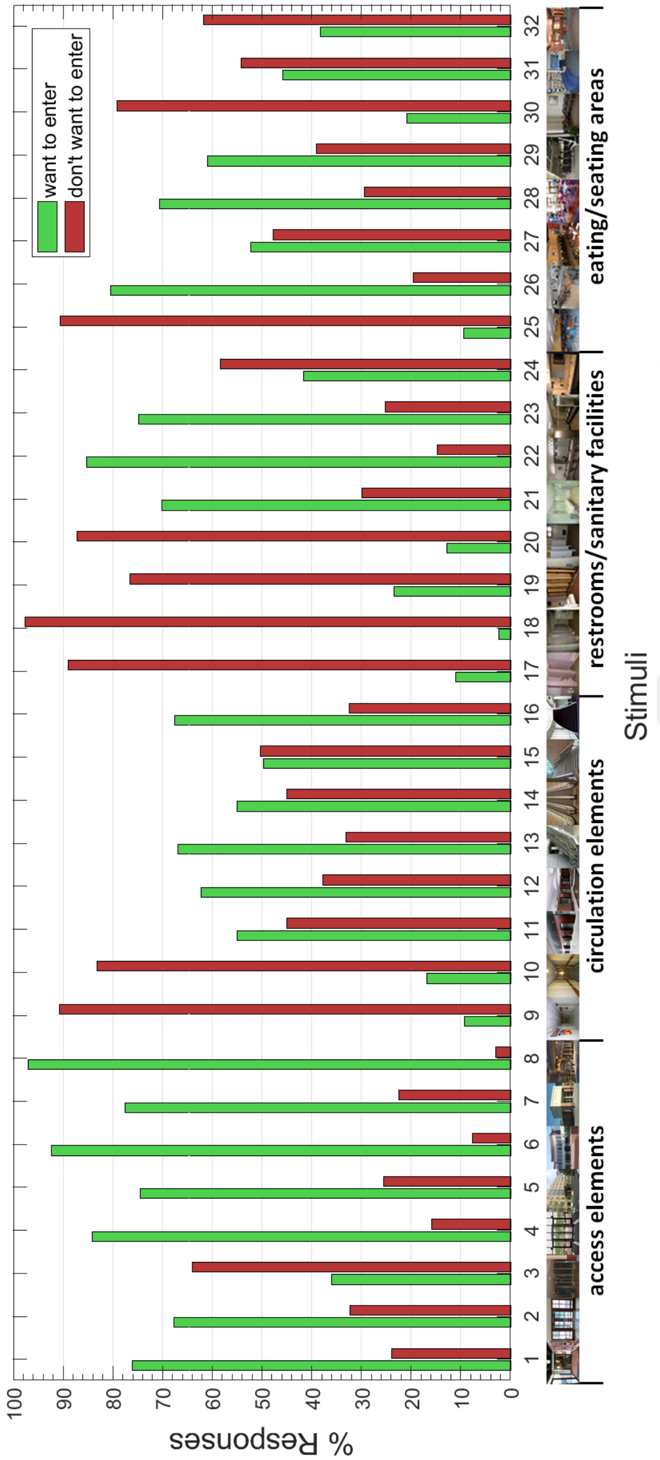

Figure A.7: **Number of approach/avoidance responses by stimuli.**

Appendix B

Permissions

ELSEVIER LICENSE
TERMS AND CONDITIONS

May 26, 2023

This Agreement between Aysu KOC ("You") and Elsevier ("Elsevier") consists of your license details and the terms and conditions provided by Elsevier and Copyright Clearance Center.

License Number	5556490299720
License date	May 26, 2023
Licensed Content Publisher	Elsevier
Licensed Content Publication	Cortex
Licensed Content Title	Two scene navigation systems dissociated by deliberate versus automatic processing
Licensed Content Author	Shosuke Suzuki,Frederik S. Kamps,Daniel D. Dilks,Michael T. Treadway
Licensed Content Date	Jul 1, 2021
Licensed Content Volume	140
Licensed Content Issue	n/a
Licensed Content Pages	11
Start Page	199
End Page	209
Type of Use	reuse in a thesis/dissertation
Portion	figures/tables/illustrations

Number of figures/tables/illustrations	1
Format	both print and electronic
Are you the author of this Elsevier article?	No
Will you be translating?	No
Title	Perception of built environments and its neural modulation by the behavioral goals of the perceiver
Institution name	Ihsan Dogramaci Bilkent University
Expected presentation date	Jul 2023
Portions	Figure 2
Requestor Location	Aysu KOC Emek mah, biskek cad, 157/6 Ankara, Cankaya 06490 Turkey Attn: Aysu KOC
Publisher Tax ID	GB 494 6272 12
Total	0.00 USD
Terms and Conditions	

INTRODUCTION

1. The publisher for this copyrighted material is Elsevier. By clicking "accept" in connection with completing this licensing transaction, you agree that the following terms and conditions apply to this transaction (along with the Billing and Payment terms and conditions established by Copyright Clearance Center, Inc. ("CCC"), at the time that you opened your Rightslink account and that are available at any time at http://myaccount.copyright.com).

GENERAL TERMS

2. Elsevier hereby grants you permission to reproduce the aforementioned material subject to the terms and conditions indicated.

3. Acknowledgement: If any part of the material to be used (for example, figures) has appeared in our publication with credit or acknowledgement to another source, permission must also be sought from that source. If such permission is not obtained then that material may not be included in your publication/copies. Suitable acknowledgement to the source must be made, either as a footnote or in a reference list at the end of your publication, as follows:

"Reprinted from Publication title, Vol /edition number, Author(s), Title of article / title of chapter, Pages No., Copyright (Year), with permission from Elsevier [OR APPLICABLE SOCIETY COPYRIGHT OWNER]." Also Lancet special credit - "Reprinted from The Lancet, Vol. number, Author(s), Title of article, Pages No., Copyright (Year), with permission from Elsevier."

4. Reproduction of this material is confined to the purpose and/or media for which permission is hereby given.

5. Altering/Modifying Material: Not Permitted. However figures and illustrations may be altered/adapted minimally to serve your work. Any other abbreviations, additions, deletions and/or any other alterations shall be made only with prior written authorization of Elsevier Ltd. (Please contact Elsevier's permissions helpdesk here). No modifications can be made to any Lancet figures/tables and they must be reproduced in full.

6. If the permission fee for the requested use of our material is waived in this instance, please be advised that your future requests for Elsevier materials may attract a fee.

7. Reservation of Rights: Publisher reserves all rights not specifically granted in the combination of (i) the license details provided by you and accepted in the course of this licensing transaction, (ii) these terms and conditions and (iii) CCC's Billing and Payment terms and conditions.

8. License Contingent Upon Payment: While you may exercise the rights licensed immediately upon issuance of the license at the end of the licensing process for the transaction, provided that you have disclosed complete and accurate details of your proposed use, no license is finally effective unless and until full payment is received from you (either by publisher or by CCC) as provided in CCC's Billing and Payment terms and conditions. If full payment is not received on a timely basis, then any license preliminarily granted shall be deemed automatically revoked and shall be void as if never granted. Further, in the event that you breach any of these terms and conditions or any of CCC's Billing and Payment terms and conditions, the license is automatically revoked and shall be void as if never granted. Use of materials as described in a revoked license, as well as any use of the materials beyond the scope of an unrevoked license, may constitute copyright infringement and publisher reserves the right to take any and all action to protect its copyright in the materials.

9. Warranties: Publisher makes no representations or warranties with respect to the licensed material.

10. Indemnity: You hereby indemnify and agree to hold harmless publisher and CCC, and their respective officers, directors, employees and agents, from and against any and all claims arising out of your use of the licensed material other than as specifically authorized pursuant to this license.

11. No Transfer of License: This license is personal to you and may not be sublicensed, assigned, or transferred by you to any other person without publisher's written permission.

12. No Amendment Except in Writing: This license may not be amended except in a writing signed by both parties (or, in the case of publisher, by CCC on publisher's behalf).

13. Objection to Contrary Terms: Publisher hereby objects to any terms contained in any purchase order, acknowledgment, check endorsement or other writing prepared by you, which terms are inconsistent with these terms and conditions or CCC's Billing and Payment terms and conditions. These terms and conditions, together with CCC's Billing and Payment terms and conditions (which are incorporated herein), comprise the entire agreement between you and publisher (and CCC) concerning this licensing transaction. In the event of any conflict between your obligations established by these terms and conditions and those established by CCC's Billing and Payment terms and conditions, these terms and conditions shall control.

14. Revocation: Elsevier or Copyright Clearance Center may deny the permissions described in this License at their sole discretion, for any reason or no reason, with a full refund payable to you. Notice of such denial will be made using the contact information provided by you. Failure to receive such notice will not alter or invalidate the denial. In no event will Elsevier or Copyright Clearance Center be responsible or liable for any costs, expenses or damage incurred by you as a result of a denial of your permission request, other than a refund of the amount(s) paid by you to Elsevier and/or Copyright Clearance Center for denied permissions.

LIMITED LICENSE

The following terms and conditions apply only to specific license types:

15. **Translation**: This permission is granted for non-exclusive world **English** rights only unless your license was granted for translation rights. If you licensed translation rights you may only translate this content into the languages you requested. A professional translator must perform all translations and reproduce the content word for word preserving the integrity of the article.

16. **Posting licensed content on any Website**: The following terms and conditions apply as follows: Licensing material from an Elsevier journal: All content posted to the web site must maintain the copyright information line on the bottom of each image; A hyper-text must be included to the Homepage of the journal from which you are licensing at http://www.sciencedirect.com/science/journal/xxxxx or the Elsevier homepage for books at http://www.elsevier.com; Central Storage: This license does not include permission for a scanned version of the material to be stored in a central repository such as that provided by Heron/XanEdu.

Licensing material from an Elsevier book: A hyper-text link must be included to the Elsevier homepage at http://www.elsevier.com . All content posted to the web site must maintain the copyright information line on the bottom of each image.

Posting licensed content on Electronic reserve: In addition to the above the following clauses are applicable: The web site must be password-protected and made available only to bona fide students registered on a relevant course. This permission is granted for 1 year only. You may obtain a new license for future website posting.

17. **For journal authors:** the following clauses are applicable in addition to the above:

Preprints:

A preprint is an author's own write-up of research results and analysis, it has not been peer-reviewed, nor has it had any other value added to it by a publisher (such as formatting, copyright, technical enhancement etc.).

Authors can share their preprints anywhere at any time. Preprints should not be added to or enhanced in any way in order to appear more like, or to substitute for, the final versions of articles however authors can update their preprints on arXiv or RePEc with their Accepted Author Manuscript (see below).

If accepted for publication, we encourage authors to link from the preprint to their formal publication via its DOI. Millions of researchers have access to the formal publications on ScienceDirect, and so links will help users to find, access, cite and use the best available version. Please note that Cell Press, The Lancet and some society-owned have different preprint policies. Information on these policies is available on the journal homepage.

Accepted Author Manuscripts: An accepted author manuscript is the manuscript of an article that has been accepted for publication and which typically includes author-incorporated changes suggested during submission, peer review and editor-author communications.

Authors can share their accepted author manuscript:

- immediately
  - via their non-commercial person homepage or blog
  - by updating a preprint in arXiv or RePEc with the accepted manuscript
  - via their research institute or institutional repository for internal institutional uses or as part of an invitation-only research collaboration work-group
  - directly by providing copies to their students or to research collaborators for their personal use
  - for private scholarly sharing as part of an invitation-only work group on commercial sites with which Elsevier has an agreement
- After the embargo period
  - via non-commercial hosting platforms such as their institutional repository
  - via commercial sites with which Elsevier has an agreement

In all cases accepted manuscripts should:

- link to the formal publication via its DOI
- bear a CC-BY-NC-ND license - this is easy to do
- if aggregated with other manuscripts, for example in a repository or other site, be shared in alignment with our hosting policy not be added to or enhanced in any way to appear more like, or to substitute for, the published journal article.

Published journal article (JPA): A published journal article (PJA) is the definitive final record of published research that appears or will appear in the journal and embodies all value-adding publishing activities including peer review co-ordination, copy-editing, formatting, (if relevant) pagination and online enrichment.

Policies for sharing publishing journal articles differ for subscription and gold open access articles:

Subscription Articles: If you are an author, please share a link to your article rather than the full-text. Millions of researchers have access to the formal publications on ScienceDirect, and so links will help your users to find, access, cite, and use the best available version.

Theses and dissertations which contain embedded PJAs as part of the formal submission can be posted publicly by the awarding institution with DOI links back to the formal publications on ScienceDirect.

If you are affiliated with a library that subscribes to ScienceDirect you have additional private sharing rights for others' research accessed under that agreement. This includes use for classroom teaching and internal training at the institution (including use in course packs and courseware programs), and inclusion of the article for grant funding purposes.

Gold Open Access Articles: May be shared according to the author-selected end-user license and should contain a CrossMark logo, the end user license, and a DOI link to the formal publication on ScienceDirect.

Please refer to Elsevier's posting policy for further information.

18. **For book authors** the following clauses are applicable in addition to the above: Authors are permitted to place a brief summary of their work online only. You are not allowed to download and post the published electronic version of your chapter, nor may you scan the printed edition to create an electronic version. **Posting to a repository:** Authors are permitted to post a summary of their chapter only in their institution's repository.

19. **Thesis/Dissertation**: If your license is for use in a thesis/dissertation your thesis may be submitted to your institution in either print or electronic form. Should your thesis be published commercially, please reapply for permission. These requirements include permission for the Library and Archives of Canada to supply single copies, on demand, of the complete thesis and include permission for Proquest/UMI to supply single copies, on demand, of the complete thesis. Should your thesis be published commercially, please reapply for permission. Theses and dissertations which contain embedded PJAs as part of the formal submission can be posted publicly by the awarding institution with DOI links back to the formal publications on ScienceDirect.

Elsevier Open Access Terms and Conditions

You can publish open access with Elsevier in hundreds of open access journals or in nearly 2000 established subscription journals that support open access publishing. Permitted third party re-use of these open access articles is defined by the author's choice of Creative Commons user license. See our open access license policy for more information.

Terms & Conditions applicable to all Open Access articles published with Elsevier:

Any reuse of the article must not represent the author as endorsing the adaptation of the article nor should the article be modified in such a way as to damage the author's honour or reputation. If any changes have been made, such changes must be clearly indicated.

The author(s) must be appropriately credited and we ask that you include the end user license and a DOI link to the formal publication on ScienceDirect.

If any part of the material to be used (for example, figures) has appeared in our publication with credit or acknowledgement to another source it is the responsibility of the user to ensure their reuse complies with the terms and conditions determined by the rights holder.

Additional Terms & Conditions applicable to each Creative Commons user license:

CC BY: The CC-BY license allows users to copy, to create extracts, abstracts and new works from the Article, to alter and revise the Article and to make commercial use of the Article (including reuse and/or resale of the Article by commercial entities), provided the user gives appropriate credit (with a link to the formal publication through the relevant DOI), provides a link to the license, indicates if changes were made and the licensor is not represented as endorsing the use made of the work. The full details of the license are available at http://creativecommons.org/licenses/by/4.0.

CC BY NC SA: The CC BY-NC-SA license allows users to copy, to create extracts, abstracts and new works from the Article, to alter and revise the Article, provided this is not done for commercial purposes, and that the user gives appropriate credit (with a link to the formal publication through the relevant DOI), provides a link to the license, indicates if changes were made and the licensor is not represented as endorsing the use made of the work. Further, any new works must be made available on the same conditions. The full details of the license are available at http://creativecommons.org/licenses/by-nc-sa/4.0.

CC BY NC ND: The CC BY-NC-ND license allows users to copy and distribute the Article, provided this is not done for commercial purposes and further does not permit distribution of the Article if it is changed or edited in any way, and provided the user gives appropriate credit (with a link to the formal publication through the relevant DOI), provides a link to the license, and that the licensor is not represented as endorsing the use made of the work. The full details of the license are available at http://creativecommons.org/licenses/by-nc-nd/4.0. Any commercial reuse of Open Access articles published with a CC BY NC SA or CC BY NC ND license requires permission from Elsevier and will be subject to a fee.

Commercial reuse includes:

- Associating advertising with the full text of the Article
- Charging fees for document delivery or access
- Article aggregation
- Systematic distribution via e-mail lists or share buttons

Posting or linking by commercial companies for use by customers of those companies.

20. **Other Conditions**:

v1.10

Questions? customercare@copyright.com.

28/05/2023

To the Institute for Human Centered Design:

I am writing to formally request permission to reproduce a figure from a book in my thesis titled “Perception of Built Environments and its Neural Modulation by the Behavioral Goals of the Perceiver”. I am currently a graduate student at Ihsan Dogramacı Bilkent University pursuing my Master’s degree in Neuroscience, and the figure is essential to support my methodology. The thesis will be submitted to Ihsan Dogramaci Bilkent University and may also be made available to the public in electronic and/or print format. It will be cited and referred in accordance with my institution’s guidelines.

The details of the figure are as follows:

- Book Title: Universal Design: A Methodological Approach
- Author of the Book: Froyen, Hubert
- Figure Number: 376
- Description of the Figure: Universal Design Users-Built Environments Model

If you decide to permit my use of this figure, please fill the section below and e-mail this document to me.
Sincerely yours,

Aysu Nur KOÇ
MSc student at Bilkent University
Department of Neuroscience

We do ___X__ do not _____ grant permission for the described content to be used for the purpose stated above.

Name : Valerie D. Fletcher, Executive Director

Address:

Date : May 28, 2023

Signature :